

## Supporting Information

### A photoswitchable rotaxane operating in monolayers on solid support

Felix B. Schwarz,<sup>[a]</sup> Thomas Heinrich,<sup>[a,b]</sup> Andreas Lippitz,<sup>[b]</sup> Wolfgang E. S. Unger,<sup>\*[b]</sup> and Christoph A. Schalley<sup>\*[a]</sup>

[a] Institut für Chemie und Biochemie der Freien Universität Berlin Takustr. 3, 14195 Berlin (Germany)

[b] Federal Institute for Materials Research and Testing, Unter den Eichen 44-46, 12203 Berlin (Germany)

### Contents

1. General methods.....	S2
2. Instrumentation.....	S2
3. Preparation and characterization of compounds.....	S3
4. Original spectra of new compounds .....	S12
5. <sup>1</sup> H NMR and IRMPD-ESI-FTICR MS spectra for the formation of <b>Rot1</b> .....	S23
6. Variable-temperature <sup>1</sup> H NMR spectra of <b>Rot1</b> .....	S26
7. Determination of binding constants .....	S27
9. Clicked surfaces .....	S27
10. Surface preparations .....	S28
11. NEXAFS and XPS.....	S29
12. Contact angle measurements .....	S34
13. References.....	S34

## 1. General methods

Reagents were purchased from Sigma-Aldrich, Alfa Aesar, ACROS or Fluka and used without further purification. Dry solvents were purchased from ACROS. Silica gel (0.04-0.063 mm; Machery-Nagel) was used for column chromatography. Ethanol (EtOH), dichloromethane (DCM), dimethylformamide (DMF), and acetonitrile (ACN) used for surface experiments were purchased from Carl Roth or VWR in HPLC grade and used as received. All reactions were carried out under argon protective atmosphere.

For XPS and NEXAFS experiments, layers were prepared on polished single-crystal Si(111) wafers purchased from Crystec GmbH, stored under argon prior to use and cut into pieces ( $\sim 1 \text{ cm}^2$ ) with a diamond cutter. Microscope glass slides, used for transmission UV/Vis spectroscopy were purchased from Thermo Scientific. All SAM, macrocycle and metal ion depositions were performed in gamma-sterilized tubes (Orange Scientific).

## 2. Instrumentation

NMR spectra were recorded on a Bruker ECX 400 ( $^1\text{H}$  at 400 MHz,  $^{13}\text{C}$  at 100 MHz) at room temperature. All chemical shifts are reported in ppm with solvent signals taken as the internal standards. Mass spectra were measured on an Agilent Technologies Ionspec QFT-7 ESI-FTICR or an Agilent 6210 ESI-TOF instrument. UV-Vis spectra were measured on a Varian Cary 50 UV-Vis spectrometer. For surface UV-Vis spectra, a spectrum of the underlying SAM was used as background and subtracted from all monolayer spectra.

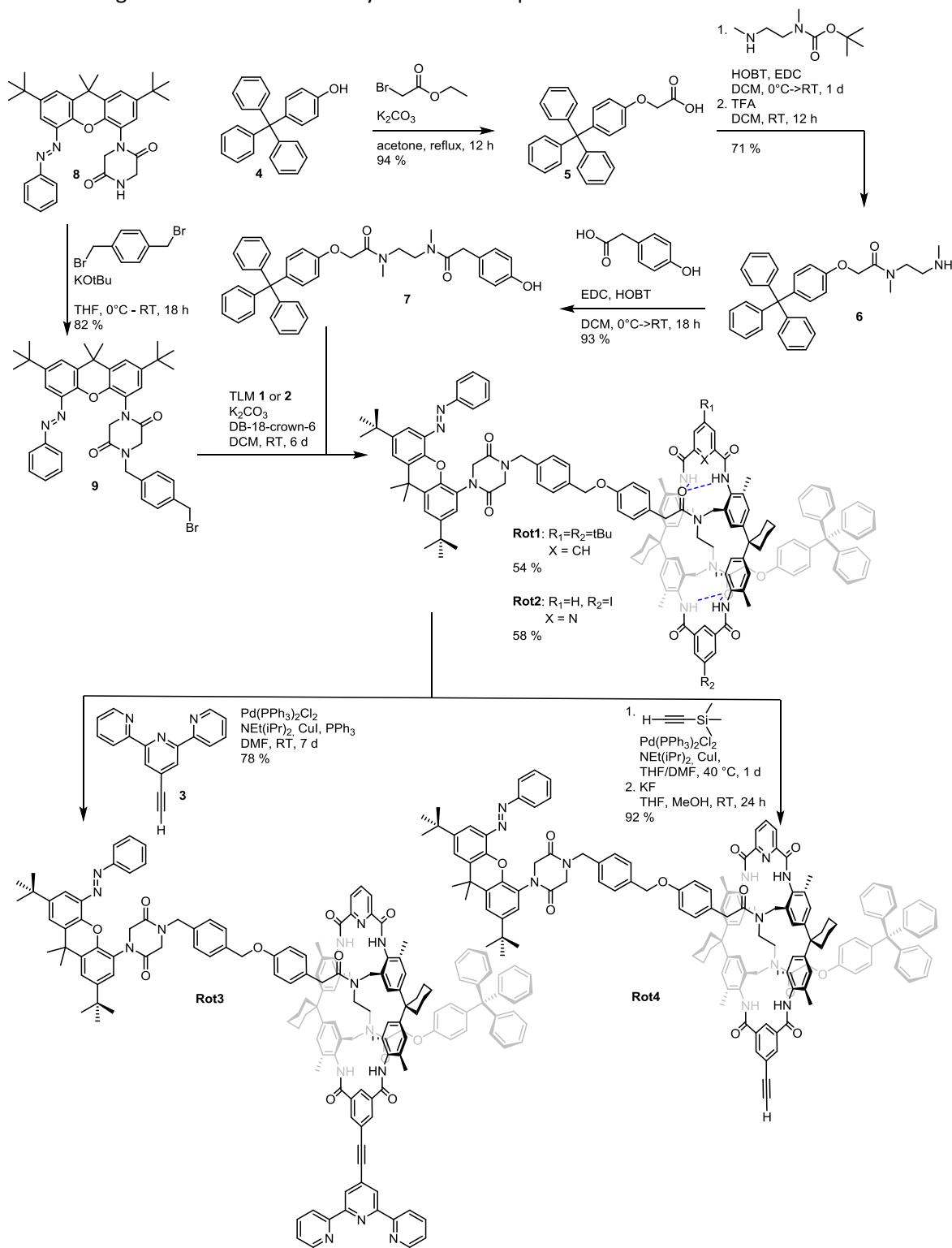
XPS and NEXAFS measurements were carried out at the HESGM CRG dipole magnet beamline at the synchrotron radiation source BESSY II (Berlin, Germany). SR XPS (synchrotron radiation XPS) N 1s, Si 2p, and C 1s data were acquired by a Scienta 3000 hemispherical electron analyser (pass energy = 50 eV) at the HE-SGM dipole magnet CRG beamline. The same beamline was used for the acquisition of all NEXAFS spectra. An emission angle of  $0^\circ$  was used for all XPS measurements. The binding energy scale of the XP spectra was corrected for static charging using an electron binding energy BE of 99.2 eV for Si 2p ( $\text{Si}^0$ ) photoemission of the silicon substrate.<sup>1</sup> Peak fitting of XP spectra was performed with a Lorentzian–Gaussian sum function peak-shape model using the Unifit 2013 software (Unifit Scientific Software GmbH, Leipzig, Germany). Peak fits and integrated peak areas were obtained after subtraction of a polynomial background. If not otherwise noted, the FWHM for component peaks in N 1s and C 1s spectra were constrained to be identical. NEXAFS spectra were acquired in the TEY (total electron yield) mode and incident angles of linearly polarized synchrotron light of  $30^\circ$  (electric field vector upright to surface plane),  $55^\circ$  and  $90^\circ$  (electric field vector parallel to the surface plane).<sup>2</sup> The resolution  $E/\Delta E$  of the monochromator at the carbonyl  $\pi^*$  resonance ( $h\nu = 287.4 \text{ eV}$ ) of CO was in the order of 2500. Raw spectra were divided by ring current and monochromator transmission function. The latter was obtained with a freshly sputtered Au sample.<sup>2</sup> Energy alignment of the energy scales was achieved by using an  $I_0$  feature referenced to a C1s  $\rightarrow \pi^*$  resonance measured with a fresh surface of HOPG (highly ordered pyrolytic graphite, Advanced Ceramic Corp., Cleveland, USA) at 285.4 eV.<sup>3</sup>

Irradiation experiments were carried out with a Thorlabs DC2200 LED driver equipped with a M365LP1 (365 nm) or M470L3 (470 nm) mounted LED.

### 3. Preparation and characterization of compounds

#### 3.1 Synthesis Overview

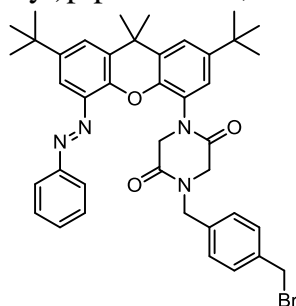
Scheme S1 gives an overview of the synthesis of compounds.



Scheme S1: Synthesis of new compounds.

Xanthene **8** was prepared as described before<sup>4</sup> and converted to axle building block **9** by attaching xylylene dibromide. Axle building block **7** was synthesised in three steps from literature known carboxylic acid **5**. Terpyridine **3**,<sup>5</sup> acid **5**<sup>6</sup> and tetralactam macrocycles **1** and **2**<sup>7</sup> were prepared according to literature procedures. Rotaxanes **Rot1** and **Rot2** were obtained in a one-step ether-rotaxane synthesis from the corresponding axle building-blocks and TLM **1** or **2**. **Rot3** functionalised with a terpyridine unit at the TLM was synthesised in one step starting from **Rot2** in a Sonogashira coupling reaction with acetylene-functionalised terpyridine **3**. Alkyne-functionalised **Rot4** was prepared likewise by Sonogashira reaction of **Rot2** with trimethylsilylacetylene followed by deprotection of the alkyne.

### 3.2 Synthesis of (*E*)-1-(4-(bromomethyl)benzyl)-4-(2,7-di-*tert*-butyl-9,9-dimethyl-5-(phenyldiazenyl)-9*H*-xanthen-4-yl)piperazine-2,5-dione



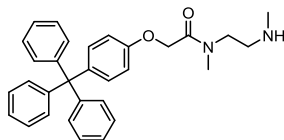
(*E*)-1-(2,7-Di-*tert*-butyl-9,9-dimethyl-5-(phenyldiazenyl)-9-xanthen-4-yl)piperazin-2,5-dion (50.0 mg, 0.093 mmol) and xylylene dibromide (245 mg, 0.930 mmol) were dissolved in dry THF (10 mL) and cooled with an ice bath to 0 °C. Potassium *tert*-butanolate (12.0 mg, 0.102 mmol) was added. The mixture was stirred for 1 h at 0 °C and for further 2.5 h at room temperature. After adding diethyl ether (50 mL), the solution was washed with distilled water (50 mL), dried over magnesium sulfate, filtered and the solvent evaporated. The residue was purified by column chromatography (silica, DCM/*n*-hexane 4:1 – DCM – DCM/EE 9:1), which afforded the product as an orange solid (55.0 mg, 0.0762 mmol, 82%).

<sup>1</sup>H NMR (400 MHz, Chloroform-*d*)  $\delta$  = 7.85 – 7.79 (m, 2H, H<sub>azobenzene</sub>), 7.57 – 7.56 (m, 1H, H<sub>xanthene</sub>), 7.51 (dd, *J* = 2.3, 0.7 Hz, 1H, H<sub>xanthene</sub>), 7.47 (m, 1H, H<sub>xanthene</sub>), 7.45 (m, 3H, H<sub>azobenzene</sub>) 7.36 (d, *J* = 7.9 Hz, 2H, H<sub>xylylene</sub>), 7.22 (d, *J* = 7.9 Hz, 2H, H<sub>xylylene</sub>), 7.15 (dd, *J* = 2.3, 0.7 Hz, 1H, H<sub>xanthene</sub>), 4.94 (bs, 2H, H<sub>piperazine-2,5-dione</sub>), 4.50 (s, 2H, H<sub>CH2</sub>), 4.27 – 4.01 (bs, 2H, H<sub>piperazine-2,5-dione</sub>), 3.85 (s, 2H, H<sub>CH2</sub>), 1.71 (s, 6H, H<sub>CH3</sub>), 1.36 (s, 9H, H<sub>*t*-bu</sub>), 1.33 (s, 9H, H<sub>*t*-bu</sub>) ppm.

<sup>13</sup>C NMR (101 MHz, Chloroform-*d*)  $\delta$  = 164.6, 164.5, 153.7, 146.6, 146.1, 145.2, 143.7, 140.6, 137.8, 135.6, 131.3, 131.3, 130.8, 129.7, 129.2, 129.2, 126.5, 125.8, 123.8, 123.1, 122.7, 112.4, 60.5, 52.8, 49.7, 49.1, 35.0, 34.9, 34.8, 33.0, 31.6, 31.5, 21.2, 14.3 ppm.

MS (ESI, pos. Mode, DCM/MeOH) *m/z*: calculated 721.2748 found 721.2741 ([M+H]<sup>+</sup>), calculated 743.2567 found 743.2563 ([M+Na]<sup>+</sup>), calculated 759.2307 found 759.2296 ([M+K]<sup>+</sup>).

### 3.3 Synthesis of *N*-methyl-*N*-(2-(methylamino)ethyl)-2-(4-tritylphenoxy)acetamide



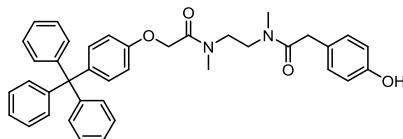
A solution of 2-(4-tritylphenoxy)acetic acid (4.50 g, 11.41 mmol), *tert*-butyl methyl(2-(methylamino)ethyl)carbamate (2.15 g, 11.41 mmol) and 1-hydroxybenzotriazole (1.93 g, 14.25 mmol) in dry DCM (80 mL) was cooled to 0 °C with an ice bath. 1-Ethyl-3-(3-dimethylaminopropyl)carbodiimide (2.21 g, 14.25 mmol) was added and the solution stirred for 2 h at 0 °C, followed by further stirring for 24 h at room temperature after the ice bath was removed. The solution was washed with saturated NaHCO<sub>3</sub> solution (1 x 80 mL), dest. water (1 x 80 mL) and brine (1 x 80 mL), dried with magnesium sulfate, filtered and the solvent evaporated. The residue was purified by column chromatography (silica, DCM->DCM/ethyl acetate 7:3), which afforded the intermediate product as a solid (5.79 g, 10.25 mmol, 89%). The intermediate product was dissolved in dry DCM (200 mL). Trifluoroacetic acid (7 mL) was added and the solution stirred for 12 h at room temperature. The solution was washed with saturated NaHCO<sub>3</sub> solution (2 x 80 mL), dried with magnesium sulfate, filtered and the solvent evaporated, which afforded the product as a colourless solid (4.40 g, 9.47 mmol, 83%).

<sup>1</sup>H NMR (500 MHz, CDCl<sub>3</sub>)  $\delta$  = 7.25 – 7.16 (m, 15H, H<sub>trityl</sub>), 7.14 – 7.09 (m, 2H, H<sub>trityl-phenol</sub>), 6.87 – 6.78 (m, 2H, H<sub>trityl-phenol</sub>), 4.72 (m, 2H, H<sub>O-CH2</sub>), 3.51 (m, 2H, H<sub>N-CH2</sub>), 3.02 (m, 3H, H<sub>CH3</sub>), 2.84 – 2.74 (m, 2H, H<sub>N-CH2</sub>), 2.43 (m, 3H, H<sub>CH3</sub>) ppm.

<sup>13</sup>C NMR (126 MHz, CDCl<sub>3</sub>)  $\delta$  = 168.8, 168.4, 156.2, 156.1, 147.0, 140.1, 139.9, 132.4, 131.2, 131.2, 127.5, 127.5, 126.0, 113.7, 113.6, 67.4, 64.4, 49.7, 49.2, 48.7, 47.2, 36.7, 35.8, 35.2, 33.7 ppm.

MS (ESI, pos. Mode, DCM/MeOH) *m/z*: calculated 465.2537 found 465.2542 ([M+H]<sup>+</sup>), calculated 487.2356 found 487.2353 ([M+Na]<sup>+</sup>), calculated 503.2095 found 503.2087 ([M+K]<sup>+</sup>).

### 3.4 Synthesis of 2-(4-hydroxyphenyl)-*N*-methyl-*N*-(2-(*N*-methyl-2-(4-tritylphenoxy)-acetamido)ethyl)acetamide



*N*-Methyl-*N*-(2-(methylamino)ethyl)-2-(4-tritylphenoxy)acetamide (2.50 g, 5.38 mmol), 4-hydroxyphenylacetic acid (818 mg, 5.38 mmol) and 1-hydroxybenzotriazole (909 mg, 6.73 mmol) were dissolved in dry DCM (80 mL). The solution was cooled to 0 °C with an ice bath. 1-Ethyl-3-(3-dimethylaminopropyl)carbodiimide (1.29 g, 6.73 mmol) was added. It was stirred for 12 h while slowly increasing the temperature to room temperature. The solution was then washed with saturated NaHCO<sub>3</sub> solution (1 x 80 mL), dest. water (1 x 80 mL) and brine (1 x 80 mL), dried with magnesium sulfate, filtered and the solvent evaporated. The residue was purified by column chromatography (silica, DCM + 3.5 % MeOH), which afforded the product as a colourless solid (2.99 g, 4.99 mmol, 93%).

<sup>1</sup>H NMR (500 MHz, CDCl<sub>3</sub>)

δ = 7.25 – 7.14 (m, 15H, H<sub>trityl</sub>), 7.11 (d, J = 9.0 Hz, 2H, H<sub>trityl-phenol</sub>), 7.03 – 6.92 (m, 2H, H<sub>phenol</sub>), 6.79 (d, J = 9.0 Hz, 2H, H<sub>trityl-phenol</sub>), 6.73 – 6.61 (m, 2H, H<sub>phenol</sub>), 5.22 – 4.63 (bs, 1H, H<sub>OH</sub>), 4.61 – 4.53 (m, 2H, H<sub>O-CH<sub>2</sub></sub>), 3.68 – 3.38 (m, 6H, H<sub>CH<sub>2</sub></sub>), 3.04 – 2.95 (m, 6H, H<sub>CH<sub>3</sub></sub>) ppm.

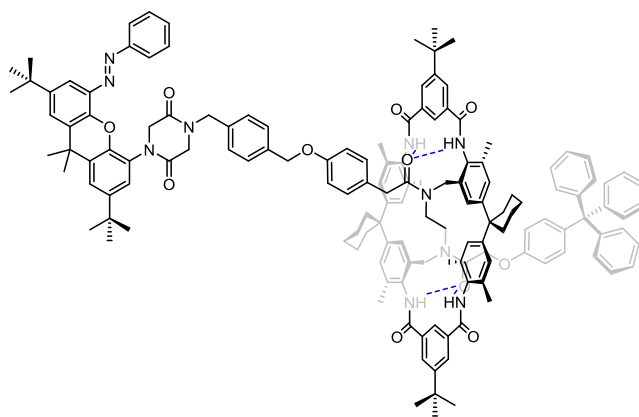
<sup>13</sup>C NMR (126 MHz, CDCl<sub>3</sub>)

δ = 173.0, 168.7, 156.0, 155.7, 147.0, 147.0, 146.9, 140.0, 132.4, 132.4, 131.2, 131.2, 130.4, 130.1, 130.0, 129.8, 127.6, 126.0, 125.6, 115.9, 113.6, 66.8, 64.4, 45.2, 45.1, 39.9, 36.4, 34.9 ppm.

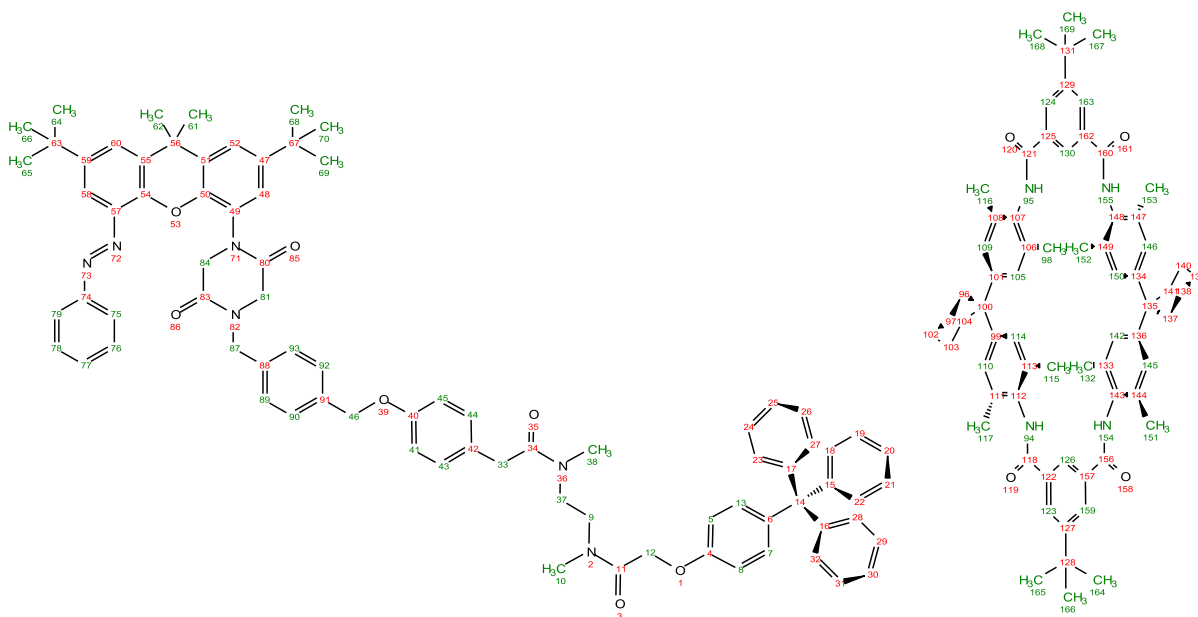
MS (ESI, pos. Mode, DCM/MeOH):

[m/z] calculated 599.2904 found 599.2907 ([M+H]<sup>+</sup>), calculated 621.2724 found 621.2725 ([M+Na]<sup>+</sup>), calculated 637.2463 found 637.2464 ([M+K]<sup>+</sup>).

### 3.5 Synthesis of **Rot1**



(E)-1-(4-(Bromomethyl)benzyl)-4-(2,7-di-*tert*-butyl-9,9-dimethyl-5-(phenyldiazenyl)-9H-xanthene-4-yl)piperazine-2,5-dione (212 mg, 0.295 mmol), 2-(4-hydroxyphenyl)-*N*-methyl-*N*-(2-(*N*-methyl-2-(4-tritylphenoxy)acetamido)ethyl)acetamide (177 mg, 0.295 mmol), TLM **1** (100 mg, 0.098 mmol), potassium carbonate (203 mg, 1.47 mmol) and dibenzo-18-crown-6 (53.0 mg, 0.147 mmol) were dissolved in dry DCM (15 mL) and stirred for 7 d at room temperature. The solution was diluted with DCM (100 mL), washed with dest. water (2 x 50 mL), dried with magnesium sulfate, filtered and the solvent evaporated. The residue was purified by column chromatography (silica, toluene/ethyl acetate 7:3 – 1:4 – toluene + 6 % MeOH), which afforded a fraction containing the rotaxane followed by a fraction containing the free axle. The fraction containing the rotaxane was further purified by preparative TLC (Silica, ethyl acetate/cyclohexane 5:7), which afforded the pure compound as an orange solid (120 mg, 0.053 mmol, 54%)



$^1\text{H}$  NMR (700 MHz, Chloroform-d)

$\delta$  = 8.61 (s, 2H, H<sub>126</sub>, 130), 8.46 (s, 4H, H<sub>94</sub>, 95, 154, 155), 8.31 (s, 4H, H<sub>123</sub>, 124, 159, 163), 7.85 (dd,  $J$  = 6.4, 1.8 Hz, 2H, H<sub>75</sub>, 79), 7.60 (d,  $J$  = 2.4 Hz, 1H, H<sub>xanthene</sub>), 7.55 (d,  $J$  = 2.3 Hz, 1H, H<sub>xanthene</sub>), 7.50 (d,  $J$  = 2.3 Hz, 1H, H<sub>xanthene</sub>), 7.49 – 7.43 (m, 3H, H<sub>76</sub>, 77, 78), 7.40 (d,  $J$  = 8.0 Hz, 2H, H<sub>90</sub>, 92), 7.29 (d,  $J$  = 9.7 Hz, 2H, H<sub>89</sub>, 93), 7.28-7.17 (m, 15 H, H<sub>trityl</sub>), 7.16 (s, d,  $J$  = 2.4 Hz, 1H, H<sub>xanthene</sub>), 7.07 (d,  $J$  = 8.9 Hz, 2H, H<sub>7</sub>, 13), 7.01 (s, 8H, H<sub>105</sub>, 109, 110, 114, 142, 145, 146, 150), 6.79 (d,  $J$  = 8.9 Hz, 2H, H<sub>43</sub>, 44), 6.77 (d,  $J$  = 8.9 Hz, 2H, H<sub>41</sub>, 45), 6.39 (d,  $J$  = 9.1 Hz, 2H, H<sub>5</sub>, 8), 5.04 (s, 2H, H<sub>46</sub>), 5.01 (bs, 2H, H<sub>84</sub>), 4.08 (bs, 2H, H<sub>81</sub>), 3.88 (s, 2H, H<sub>12</sub>), 3.86 (s, 2H, H<sub>87</sub>), 3.10 (s, 2H, H<sub>33</sub>), 2.41 (s, 3H, H<sub>10</sub>), 2.33 (bs, 6H, H<sub>cyclohexyl</sub>), 2.30 (s, 3H, H<sub>38</sub>), 2.09 (s, 24H, H<sub>98</sub>, 115, 116, 117, 132, 151, 152, 153), 2.05 – 1.97 (m, 4H, H<sub>9</sub>, 37), 1.75 (bs, 6H, H<sub>61</sub>, 62), 1.66 (bs, 10H, H<sub>cyclohexyl</sub>), 1.53 (bs, 4H, H<sub>cyclohexyl</sub>), 1.43 (s, 18H, H<sub>164</sub>, 165, 166, 167, 168, 169), 1.40 (s, 9H, H<sub>68</sub>, 69, 70), 1.37 (s, 9H, H<sub>64</sub>, 65, 66) ppm.

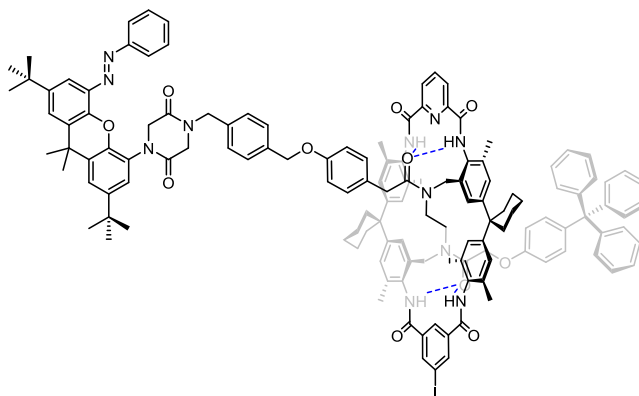
$^{13}\text{C}$  NMR (176 MHz, Chloroform-d)

$\delta$  = 173.0, 168.5, 165.8, 164.6, 164.5, 158.0, 155.0, 153.7, 153.6, 148.1, 146.7, 146.6, 146.2, 145.2, 143.7, 141.3, 140.6, 136.7, 135.3, 134.3, 132.5, 131.9, 131.4, 131.3, 131.1, 130.8, 129.2, 129.1, 129.0, 128.1, 127.7, 126.6, 126.2, 125.8, 125.4, 123.8, 123.1, 123.1, 122.7, 115.4, 113.3, 112.4, 69.8, 65.8, 64.4, 52.8, 49.6, 49.1, 45.0, 43.4, 43.3, 39.6, 35.8, 35.6, 35.5, 35.1, 35.0, 34.8, 34.1, 31.6, 31.6, 31.4, 26.4, 22.9, 19.1 ppm.

MS (ESI, pos. Mode, DCM/MeOH)

$m/z$ : calculated 2256.2497 found 2256.2492 ( $[\text{M}+\text{H}]^+$ ).

### 3.6 Synthesis of **Rot2**



(*E*)-1-(4-(Bromomethyl)benzyl)-4-(2,7-di-*tert*-butyl-9,9-dimethyl-5-(phenyldiazenyl)-9*H*-xanthene-4-yl)piperazine-2,5-dione (175 mg, 0.240 mmol), 2-(4-hydroxyphenyl)-*N*-methyl-*N*-(2-(*N*-methyl-2-(4-tritylphenoxy)acetamido)ethyl)acetamide (145 mg, 0.240 mmol), TLM **2** (100 mg, 0.097 mmol), potassium carbonate (134 mg, 0.97 mmol) and dibenzo-18-crown-6 (35.0 mg, 0.097 mmol) were dissolved in dry DCM (15 mL) and stirred for 7 d at room temperature. The solution was diluted with DCM (100 mL), washed with dest. water (2 x 50 mL), dried with magnesium sulfate, filtered and the solvent evaporated. The residue was purified by column chromatography (silica, -hexane/ethyl acetate 2:1 – ethyl acetate), which afforded a fraction containing the rotaxane followed by a fraction containing the free axle. The fraction containing the rotaxane was further purified by preparative TLC (silica, ethyl acetate/cyclohexane 5:7), which afforded the pure compound as an orange solid (128 mg, 0.056 mmol, 58%).

$^1\text{H}$  NMR (700 MHz, Chloroform-*d*)  $\delta$  = 10.38 (s, 2H,  $\text{H}_{\text{NH}}$ ), 8.54 (s, 1H,  $\text{H}_{\text{isophthal}}$ ), 8.46 (d,  $J$  = 1.5 Hz, 2H,  $\text{H}_{\text{isophthal}}$ ), 8.45 (m, 2H,  $\text{H}_{\text{NH}}$ ), 8.36 (s, 2H,  $\text{H}_{\text{isophthal}}$ ), 8.10 (t,  $J$  = 7.8 Hz, 1H,  $\text{H}_{\text{isophthal}}$ ), 7.82 (dd,  $J$  = 7.9, 1.8 Hz, 2H,  $\text{H}_{\text{azobenzene}}$ ), 7.57 (d,  $J$  = 2.4 Hz, 1H,  $\text{H}_{\text{xanthene}}$ ), 7.52 (d,  $J$  = 2.2 Hz, 1H,  $\text{H}_{\text{xanthene}}$ ), 7.47 (d,  $J$  = 2.2 Hz, 1H,  $\text{H}_{\text{xanthene}}$ ), 7.46 – 7.42 (m, 3H,  $\text{H}_{\text{azobenzene}}$ ), 7.40 (d,  $J$  = 8.4 Hz, 2H,  $\text{H}_{\text{phenyl}}$ ), 7.27 (d,  $J$  = 7.5 Hz, 2H,  $\text{H}_{\text{phenyl}}$ ), 7.26 – 7.23 (m, 5H,  $\text{H}_{\text{trityl}}$ ), 7.21 – 7.15 (m, 10H,  $\text{H}_{\text{trityl}}$ ), 7.15 (d,  $J$  = 2.2 Hz, 1H,  $\text{H}_{\text{xanthene}}$ ), 7.07 (d,  $J$  = 9.1 Hz, 2H,  $\text{H}_{\text{phenyl}}$ ), 6.98 (s, 4H,  $\text{H}_{\text{aryl TLM}}$ ), 6.95 (s, 4H,  $\text{H}_{\text{aryl TLM}}$ ), 6.71 (d,  $J$  = 8.8 Hz, 2H,  $\text{H}_{\text{phenyl}}$ ), 6.55 (d,  $J$  = 8.9 Hz, 2H,  $\text{H}_{\text{phenyl}}$ ), 6.43 (d,  $J$  = 9.1 Hz, 2H,  $\text{H}_{\text{phenyl}}$ ), 5.03 (s, 2H,  $\text{H}_{\text{CH}_2}$ ), 5.13 – 4.87 (br, 2H,  $\text{H}_{\text{diketopiperazine}}$ ), 4.17 (s, 2H,  $\text{H}_{\text{CH}_2}$ ), 4.25 – 4.01 (br, 2H,  $\text{H}_{\text{diketopiperazine}}$ ), 3.85 (s, 2H,  $\text{H}_{\text{CH}_2}$ ), 3.28 (s, 2H,  $\text{H}_{\text{CH}_2}$ ), 2.42 – 2.23 (m, 12H,  $\text{H}_{\text{CH}_3}$ ), 2.16 (m, 2H,  $\text{H}_{\text{CH}_2}$  diamide), 2.12 (s, 12H,  $\text{H}_{\text{CH}_3}$  TLM), 2.08 – 2.03 (m, 2H,  $\text{H}_{\text{CH}_2}$  diamide), 1.98 (s, 12H,  $\text{H}_{\text{CH}_2}$  TLM), 1.78 – 1.70 (m, 10H,  $\text{H}_{\text{cyclohexyl}}$ ), 1.62 – 1.56 (m, 6H,  $\text{H}_{\text{cyclohexyl}}$ ), 1.54 – 1.48 (m, 4H,  $\text{H}_{\text{cyclohexyl}}$ ), 1.37 (s, 9H,  $\text{H}_{\text{t-Bu}}$ ), 1.34 (s, 9H,  $\text{H}_{\text{t-Bu}}$ ) ppm.

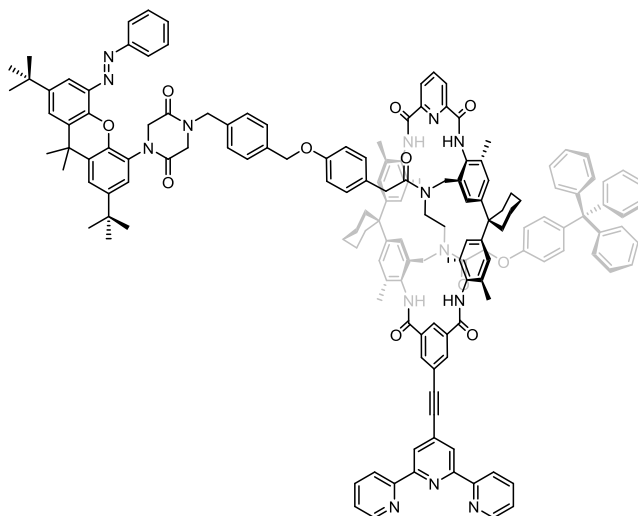
$^{13}\text{C}$  NMR (176 MHz, Chloroform-*d*)  $\delta$  = 172.7, 168.8, 164.5, 164.5, 164.5, 162.0, 157.8, 155.2, 153.6, 148.9, 146.7, 146.6, 146.1, 145.2, 143.7, 141.1, 140.6, 140.6, 139.3, 136.7, 136.4, 135.3, 135.2, 134.8, 132.6, 131.7, 131.4, 131.3, 131.3, 131.1, 131.1, 130.8, 129.2, 129.1, 128.0, 127.7, 126.6, 126.3, 126.2, 126.1, 125.8, 125.5, 125.1, 123.8, 123.1, 122.9, 122.7, 119.9, 115.2, 113.3, 112.4, 95.6, 69.8, 66.3, 64.4, 52.8, 49.6, 49.1, 45.6, 44.9, 44.9, 43.8, 43.6, 41.5, 40.3, 36.2, 36.1, 36.0, 35.9, 35.1, 35.0, 34.8, 34.8, 34.8, 34.6,

31.8, 31.7, 31.6, 31.6, 31.5, 31.2, 31.1, 29.2, 27.8, 27.0, 26.4, 25.4, 22.9, 22.9, 22.8, 22.7, 20.8, 20.6, 19.6, 19.3, 19.1, 18.9, 18.9, 14.5, 14.2, 11.6, 1.1 ppm.

MS (ESI, pos. Mode, DCM/ACN)

m/z: calculated 2271.0164 found 2271.0182 ( $[M+H]^+$ ), m/z: calculated 2292.9984 found 2293.0027 ( $[M+Na]^+$ ), m/z: calculated 2308.9723 found 2308.9734 ( $[M+K]^+$ ), m/z: calculated 1147.0028 found 1147.0055 ( $[M+H+Na]^{++}$ ), m/z: ber. 1154.9898 found 1154.9885 ( $[M+H+K]^{++}$ ), m/z: calculated 1157.9938 found 1157.9973 ( $[M+2 Na]^{++}$ ), m/z: calculated 1165.9808 found 1165.9831 ( $[M+H+Na]^{++}$ ).

### 3.7 Synthesis of **Rot3**



**Rot2** (100 mg, 0.044 mmol), 4'-ethynyl-2,2':6',2''-terpyridine (22.6 mg, 0.088 mmol), bis(triphenylphosphine)palladium(II) dichloride (3.08 mg, 0.004 mmol), copper(I) iodide (0.84 mg, 4.4  $\mu$ mol) and triphenylphosphine (4.00 mg, 0.015 mmol) were dissolved in dry DMF (16 mL) and dry diisopropylethylamine (4 mL). The solution was degassed with an argon stream for about 5 min and stirred at room temperature for 5 d. 4'-Ethynyl-2,2':6',2''-terpyridine (11.3 mg, 0.044 mmol), bis(triphenylphosphine)palladium(II) dichloride (3.08 mg, 0.004 mmol) and copper(I) iodide (0.84 mg, 4.4  $\mu$ mol) were added and the solution stirred for further 2 d. The solvents were evaporated and the residue was dissolved in DCM (10 mL) and filtered over a short column (neutral alox, DCM + 8% MeOH + 4% TEA). The solvents were evaporated and the residue was dissolved in DCM (100 mL), washed with dest. water (2 x 50 mL), dried with magnesium sulfate, filtered and the solvent evaporated. The residue was purified by dialysis (MWCO 1000, DCM/MeOH 2:1, 14 h, 4 h), which afforded the product as an orange solid.

$^1\text{H}$  NMR (700 MHz, Chloroform-d)

$\delta$  = 10.39 (s, 2H,  $H_{\text{NH}}$ ), 8.77 – 8.74 (m, 2H,  $H_{\text{terpyridine}}$ ), 8.64 (d, J = 7.7 Hz, 2H,  $H_{\text{terpyridine}}$ ), 8.57 (s, 2H,  $H_{\text{terpyridine}}$ ), 8.47 – 8.43 (m, 2H,  $H_{\text{isophthal}}$ ), 8.40 (s, 2H,  $H_{\text{NH}}$ ), 8.37 – 8.33 (m, 1H,  $H_{\text{isophthal}}$ ), 8.32 (d, J = 1.5 Hz, 1H,  $H_{\text{isophthal}}$ ), 8.11 (t, J = 7.8 Hz, 2H,  $H_{\text{terpyridine}}$ ), 7.90 (t, J = 7.1 Hz, 2H,  $H_{\text{isophthal}}$ ), 7.79 (d, J = 6.9 Hz, 2H,  $H_{\text{azobenzene}}$ ), 7.56 (d, J = 2.4 Hz, 1H,  $H_{\text{xanthene}}$ ), 7.51 (d, J = 2.4 Hz, 1H,  $H_{\text{xanthene}}$ ), 7.46 (d, J = 2.2 Hz, 1H,  $H_{\text{xanthene}}$ ), 7.44 – 7.40 (m, 3H,  $H_{\text{azobenzene}}$ ), 7.41 – 7.37 (m, 2H,  $H_{\text{terpyridine}}$ ), 7.37 (d, J = 8.1 Hz, 2H,  $H_{\text{phenyl}}$ ), 7.30 – 7.26 (m, 2H,  $H_{\text{phenyl}}$ ), 7.25 – 7.13 (m, 15H,  $H_{\text{trityl}}$ ), 7.13 (d, J = 2.2 Hz, 1H,  $H_{\text{xanthene}}$ ), 7.06 (d, J = 9.1 Hz, 2H,  $H_{\text{phenyl}}$ ), 6.99 (s, 4H,  $H_{\text{aryl TLM}}$ ), 6.96 (s, 4H,  $H_{\text{aryl TLM}}$ ), 6.72 (d,

$J = 8.6$  Hz, 2H,  $H_{\text{phenyl}}$ ), 6.58 (d,  $J = 8.2$  Hz, 2H,  $H_{\text{phenyl}}$ ), 6.45 (d,  $J = 9.1$  Hz, 2H,  $H_{\text{phenyl}}$ ), 5.03 (s, 2H,  $H_{\text{CHe}}$ ), 5.10 – 4.76 (br, 2H,  $H_{\text{diketopiperazine}}$ ), 4.32 – 3.98 (br, 2H,  $H_{\text{diketopiperazine}}$ ), 4.17 (s, 2H,  $H_{\text{CH}_2}$ ), 3.80 (s, 2H,  $H_{\text{CH}_2}$ ), 3.29 (s, 2H,  $H_{\text{CH}_2}$ ), 2.37 (s, 6H,  $H_{\text{CH}_3}$  xanthene), 2.36 – 2.22 (m, 6H,  $H_{\text{CH}_3}$  diamide), 2.21 – 2.15 (m, 2H,  $H_{\text{CH}_2}$  diamide), 2.13 (s, 12H,  $H_{\text{CH}_3 \text{ TLM}}$ ), 2.01 (s, 12H,  $H_{\text{CH}_3 \text{ TLM}}$ ), 1.96 – 1.91 (m, 2H,  $H_{\text{CH}_2}$  diamide), 1.69 (m, 10H,  $H_{\text{cyclohexyl}}$ ), 1.59 (m, 6H,  $H_{\text{cyclohexyl}}$ ), 1.52 – 1.43 (m, 4H,  $H_{\text{cyclohexyl}}$ ), 1.36 (s, 9H,  $H_{\text{t-Bu}}$ ), 1.32 (s, 9H,  $H_{\text{t-Bu}}$ ) ppm.

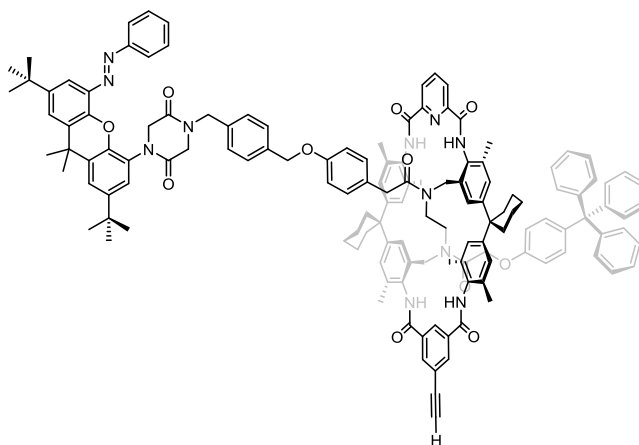
$^{13}\text{C}$  NMR (176 MHz, Chloroform- $d$ )

$\delta = 172.7, 168.7, 165.1, 164.5, 164.5, 162.0, 157.8, 155.9, 155.8, 155.6, 155.4, 155.3, 155.3, 154.5, 153.8, 153.5, 149.4, 148.9, 148.1, 147.8, 146.9, 146.7, 146.5, 146.1, 146.1, 145.2, 143.7, 143.4, 141.9, 141.1, 140.6, 140.5, 140.3, 140.0, 139.3, 137.0, 137.0, 136.7, 136.5, 136.4, 135.4, 135.2, 134.9, 134.7, 132.7, 132.5, 132.2, 132.1, 131.6, 131.6, 131.5, 131.3, 131.3, 131.1, 130.8, 129.3, 129.2, 129.1, 128.8, 128.7, 128.7, 128.6, 128.3, 128.0, 128.0, 127.9, 127.7, 126.6, 126.5, 126.1, 126.1, 125.8, 125.5, 125.1, 124.7, 124.3, 124.2, 123.8, 123.6, 123.1, 123.0, 122.7, 122.7, 121.3, 119.8, 115.1, 113.3, 112.3, 91.9, 89.5, 69.8, 66.3, 64.4, 52.8, 49.6, 49.1, 45.9, 44.9, 43.8, 43.7, 40.2, 36.1, 35.9, 35.1, 35.0, 34.9, 34.8, 34.8, 34.5, 31.6, 31.5, 31.2, 29.8, 26.4, 22.9, 19.3, 19.0, 18.9, 8.7, 1.1$  ppm.

MS (ESI, pos. Mode, DCM/ACN)

$m/z$ : calculated 2422.1814 found 2422.1807 ( $[M+Na]^+$ ),  $m/z$ : calculated 1211.5943 found 1211.5929 ( $[M+H+Na]^{++}$ ),  $m/z$ : calculated 1222.5853 found 1211.5878 ( $[M+2Na]^{++}$ ).

### 3.8 Synthesis of **Rot4**



In a pressure tube, **Rot2** (100 mg, 0.044 mmol), trimethylsilylacetylene (13.0 mg, 0.132 mmol), bis(triphenylphosphine)palladium(II) dichloride (3.08 mg, 4.4  $\mu\text{mol}$ ) and copper(I) iodide (0.84 mg, 4.4  $\mu\text{mol}$ ) were dissolved in a mixture of dry THF (8 mL), dry DMF (2 mL) and dry diisopropylethylamine (6 mL) and stirred at 40 °C for 24 h. The solution was diluted with DCM (50 mL), washed with dest. water (2 x 50 mL) and brine (50 mL), dried with magnesium sulfate, filtered and the solvent evaporated. The residue was purified by preparative TLC (silica, ethyl acetate/*n*-hexane 6:5), which afforded the TMS-protected intermediate as an orange solid. The intermediate and potassium fluoride (26.0 mg, 0.44 mmol) were dissolved in THF (8 mL) and MeOH (6 mL) and stirred for 24 h at room temperature. The solvents were evaporated and the residue dissolved in

DCM (50 mL). The solution was washed with dest. water (2 x 50 mL), dried with magnesium sulfate, filtered and the solvent evaporated. The residue was purified by preparative TLC (silica, ethyl acetate/cyclohexane 5:7), which afforded the product as an orange solid (87.7 mg, 0.04 mmol, 92 %).

<sup>1</sup>H NMR (500 MHz, Chloroform-d)  $\delta$  = 10.40 (s, 2H, H<sub>NH</sub>), 8.57 (s, 1H, H<sub>isophthal</sub>), 8.48 (d, J = 7.7 Hz, 2H, H<sub>isophthal</sub>), 8.40 – 8.37 (m, 2H, H<sub>NH</sub>), 8.26 (d, J = 1.6 Hz, 2H, H<sub>isophthal</sub>), 8.13 (t, J = 7.8 Hz, 1H, H<sub>isophthal</sub>), 7.86 – 7.82 (m, 2H, H<sub>azobenzene</sub>), 7.59 (d, J = 2.4 Hz, 1H, H<sub>xanthene</sub>), 7.54 (d, J = 2.4 Hz, 1H, H<sub>xanthene</sub>), 7.50 (d, J = 2.4 Hz, 1H, H<sub>xanthene</sub>), 7.48 – 7.44 (m, 3H, H<sub>azobenzene</sub>), 7.42 (d, J = 8.4 Hz, 2H, H<sub>phenyl</sub>), 7.29 (d, J = 6.1 Hz, 2H, H<sub>phenyl</sub>), 7.28 – 7.25 (m, 5H, H<sub>trityl</sub>), 7.26 – 7.13 (m, 10H, H<sub>trityl</sub>), 7.19 (d, J = 2.4 Hz, 1H, H<sub>xanthene</sub>), 7.09 (d, J = 9.0 Hz, 2H, H<sub>phenyl</sub>), 7.00 (s, 4H, H<sub>aryl TLM</sub>), 6.97 (s, 4H, H<sub>aryl TLM</sub>), 6.72 (d, J = 8.7 Hz, 2H, H<sub>phenyl</sub>), 6.59 (d, J = 8.5 Hz, 2H, H<sub>phenyl</sub>), 6.46 (d, J = 9.1 Hz, 2H, H<sub>phenyl</sub>), 5.04 (s, 2H, H<sub>CH<sub>2</sub></sub>), 5.22 – 4.78 (br, 2H, H<sub>diketopiperazine</sub>), 4.17 (s, 2H, H<sub>CH<sub>2</sub></sub>), 4.33 – 3.93 (br, 2H, H<sub>diketopiperazine</sub>), 3.87 (s, 2H, H<sub>CH<sub>2</sub></sub>), 3.31 (s, 2H, H<sub>CH<sub>2</sub></sub>), 3.17 (s, 1H, H<sub>acetylene</sub>), 2.41 – 2.25 (m, 12H, H<sub>CH<sub>3</sub></sub>), 2.19 (m, 2H, H<sub>CH<sub>2</sub> diamide</sub>), 2.15 (s, 12H, H<sub>CH<sub>3</sub> TLM</sub>), 2.11 (m, 2H, H<sub>CH<sub>2</sub> diamide</sub>), 2.01 (s, 12H, H<sub>CH<sub>3</sub> TLM</sub>), 1.72 (m, 10H, H<sub>cyclohexyl</sub>), 1.61 (m, 6H, H<sub>cyclohexyl</sub>), 1.54 – 1.47 (m, 4H, H<sub>cyclohexyl</sub>), 1.39 (s, 9H, H<sub>t-Bu</sub>), 1.36 (s, 9H, H<sub>t-Bu</sub>) ppm.

<sup>13</sup>C NMR (126 MHz, Chloroform-d)  $\delta$  = 172.7, 168.7, 165.1, 164.5, 162.0, 157.8, 155.3, 153.6, 148.9, 148.0, 147.8, 146.7, 146.6, 146.1, 145.2, 143.7, 141.0, 140.6, 139.3, 136.7, 135.3, 135.2, 134.9, 134.8, 132.5, 131.6, 131.5, 131.3, 131.3, 131.1, 130.8, 129.3, 129.2, 129.1, 128.0, 127.7, 127.0, 126.6, 126.5, 126.1, 126.1, 125.8, 125.4, 125.1, 124.5, 123.8, 123.0, 122.7, 115.1, 113.2, 112.4, 82.0, 79.5, 69.7, 66.3, 64.4, 53.5, 52.8, 49.6, 49.1, 44.9, 43.8, 43.6, 40.2, 36.1, 35.9, 35.9, 35.0, 34.9, 34.8, 34.7, 31.6, 31.5, 26.3, 22.9, 22.8, 19.3, 18.9 ppm.

MS (ESI, pos. Mode, DCM/ACN) m/z: calculated 2191.1017 found 2191.0848 ([M+Na]<sup>+</sup>), m/z: calculated 1104.0415 found 1104.0358 ([M+H+K]<sup>++</sup>), m/z: calculated 1107.0455 found 1107.0455 ([M+2Na]<sup>++</sup>), m/z: calculated 1115.0324 found 1115.0321 ([M+Na+K]<sup>++</sup>).

## 4. Original spectra of new compounds

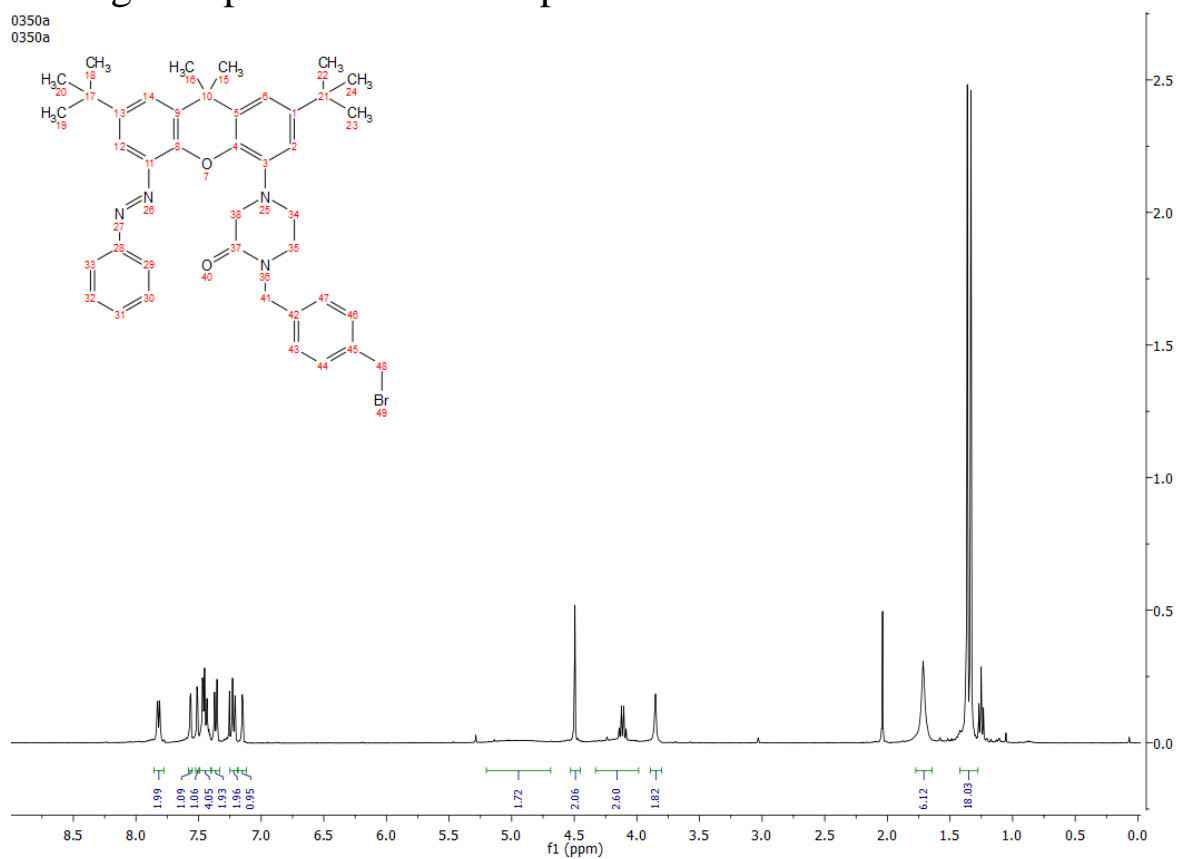


Figure S1:  $^1\text{H}$  NMR spectrum (298 K,  $\text{CDCl}_3$ ) of 9.

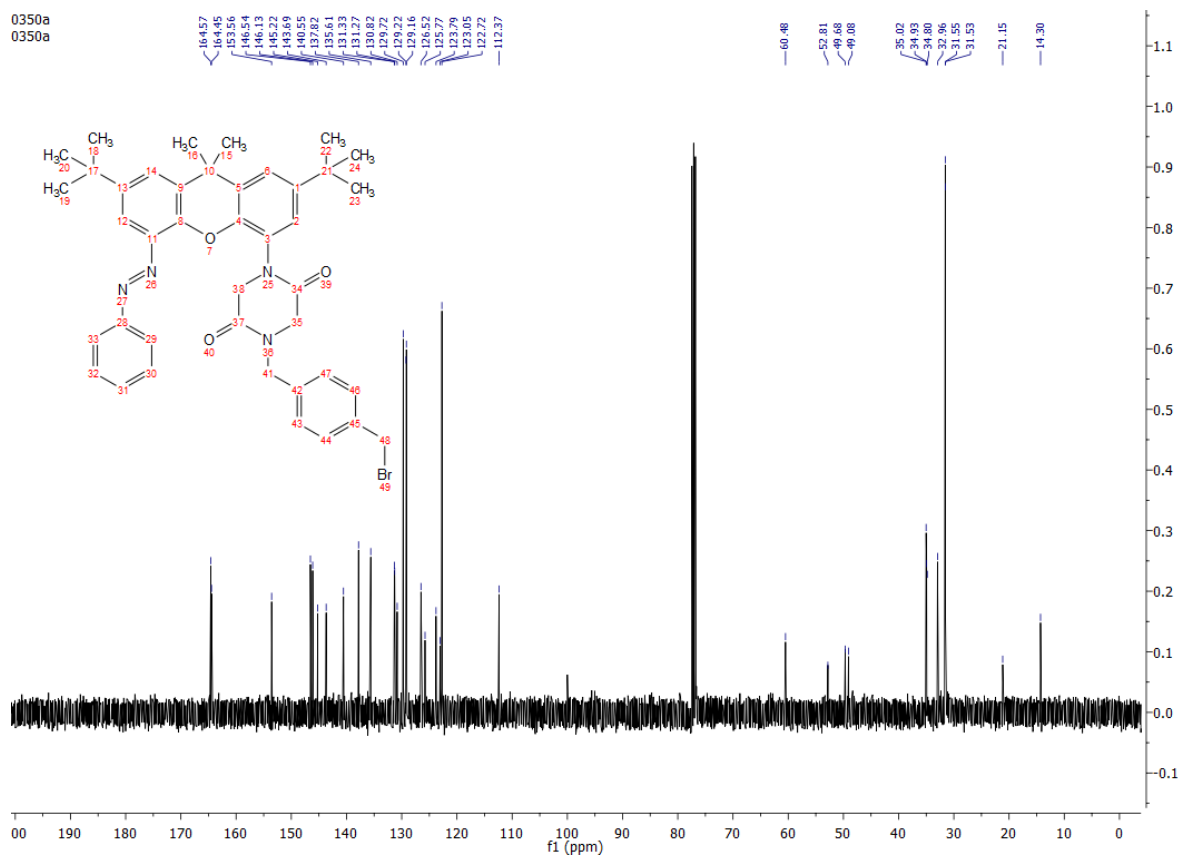


Figure S2:  $^{13}\text{C}$  NMR spectrum (298 K,  $\text{CDCl}_3$ ) of 9.

Sample Name	0350	Position	Vial 1	Instrument Name	Instrument 1	User Name	
Inj Vol	5	InjPosition		SampleType	Sample	IRM Calibration Status	Success
Data Filename	3442_Schwarz_0350.d	ACQ Method		Comment	DCM/MeOH	Acquired Time	7/8/2016 10:33:30 AM

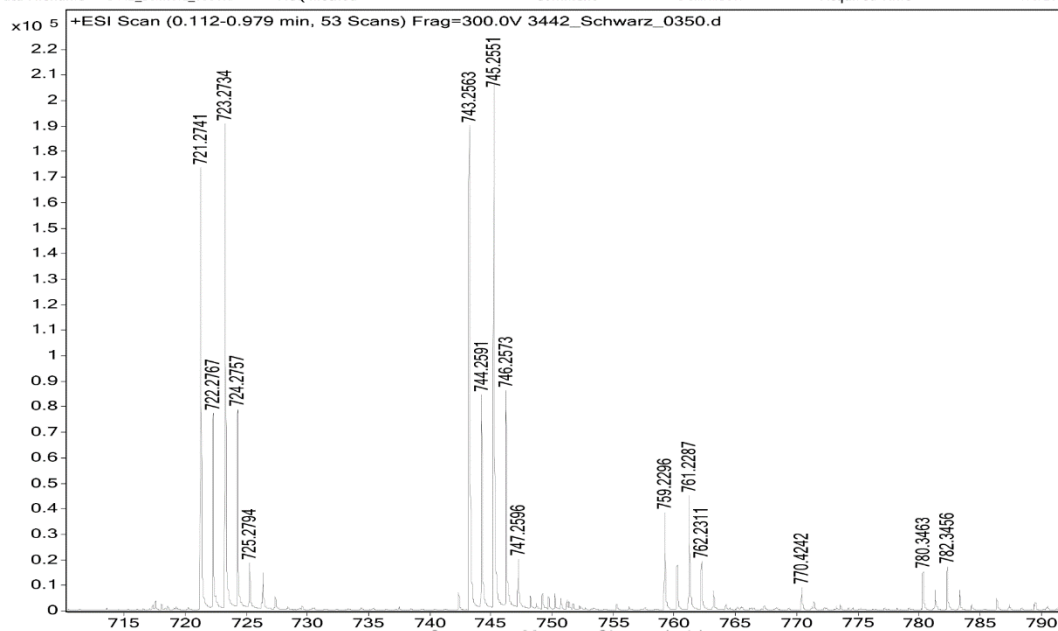


Figure S3: ESI-MS spectrum (DCM, MeOH) of 9.

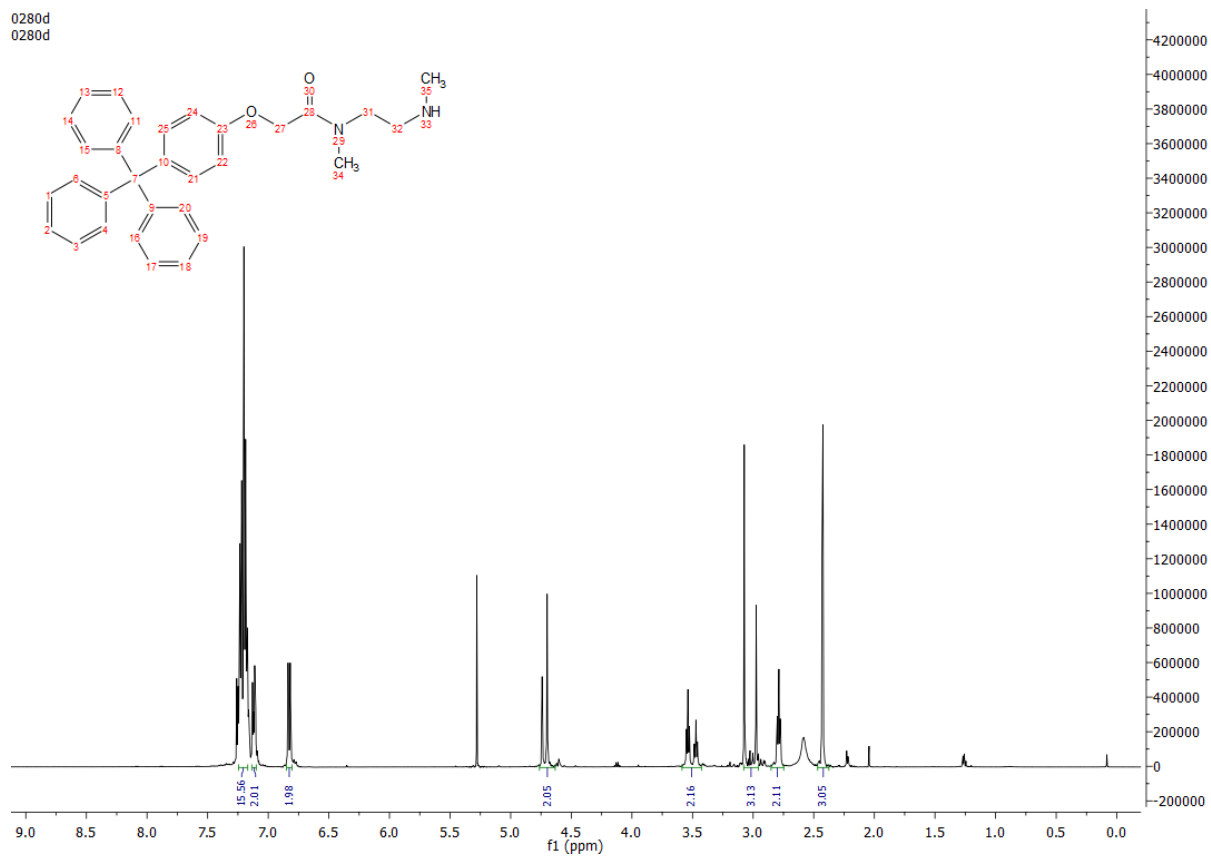


Figure S4: <sup>1</sup>H NMR spectrum (298 K, CDCl<sub>3</sub>) of 6.

0280d  
0280d

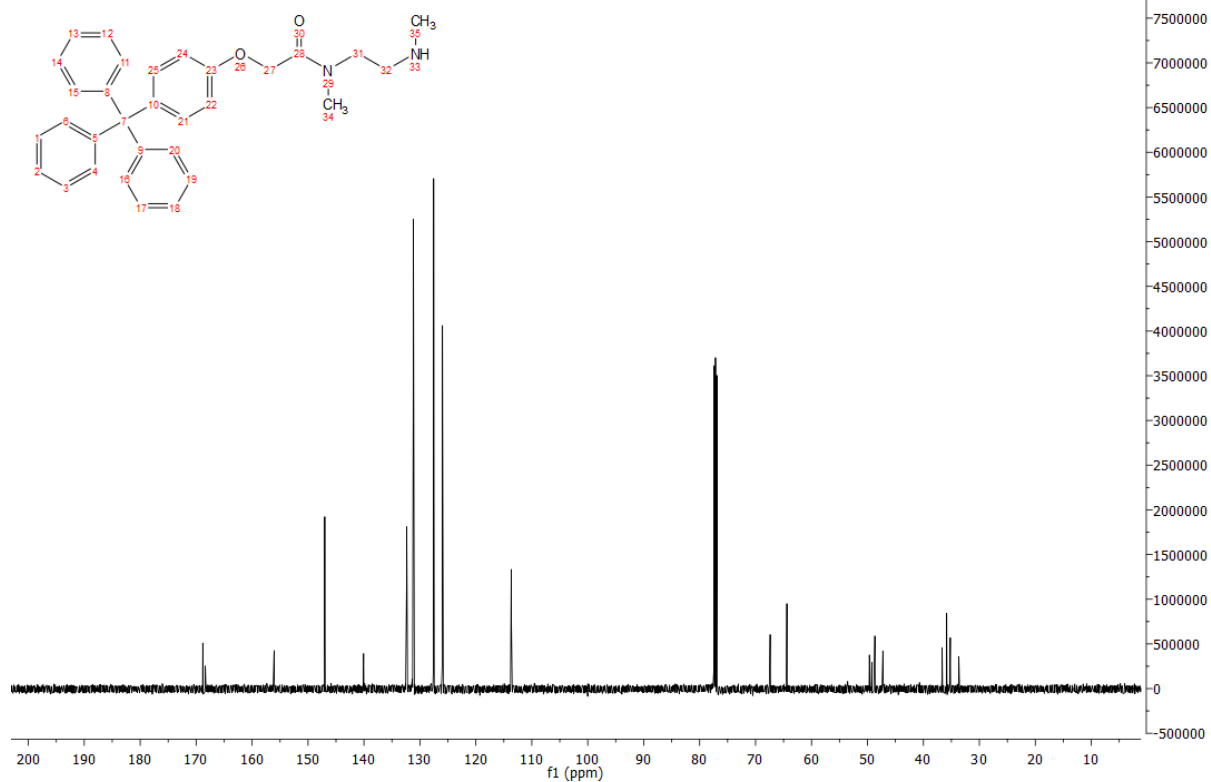


Figure S5:  $^{13}\text{C}$  NMR spectrum (298 K,  $\text{CDCl}_3$ ) of 6.

Sample Name	0280	Position	Vial 1	Instrument Name	Instrument 1	User Name
Inj Vol	5	InjPosition		SampleType	Sample	IRM Calibration Status
Data Filename	3443_Schwarz_0280.d	ACQ Method		Comment	DCM/MeOH	Acquired Time
						Success
						7/8/2016 10:41:47 AM

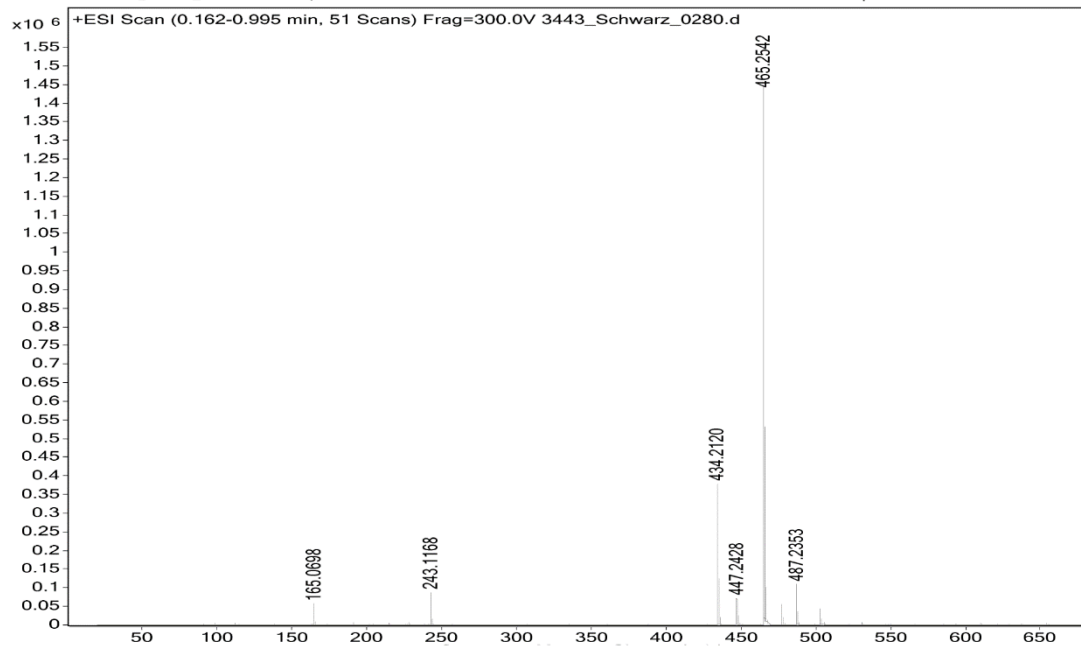
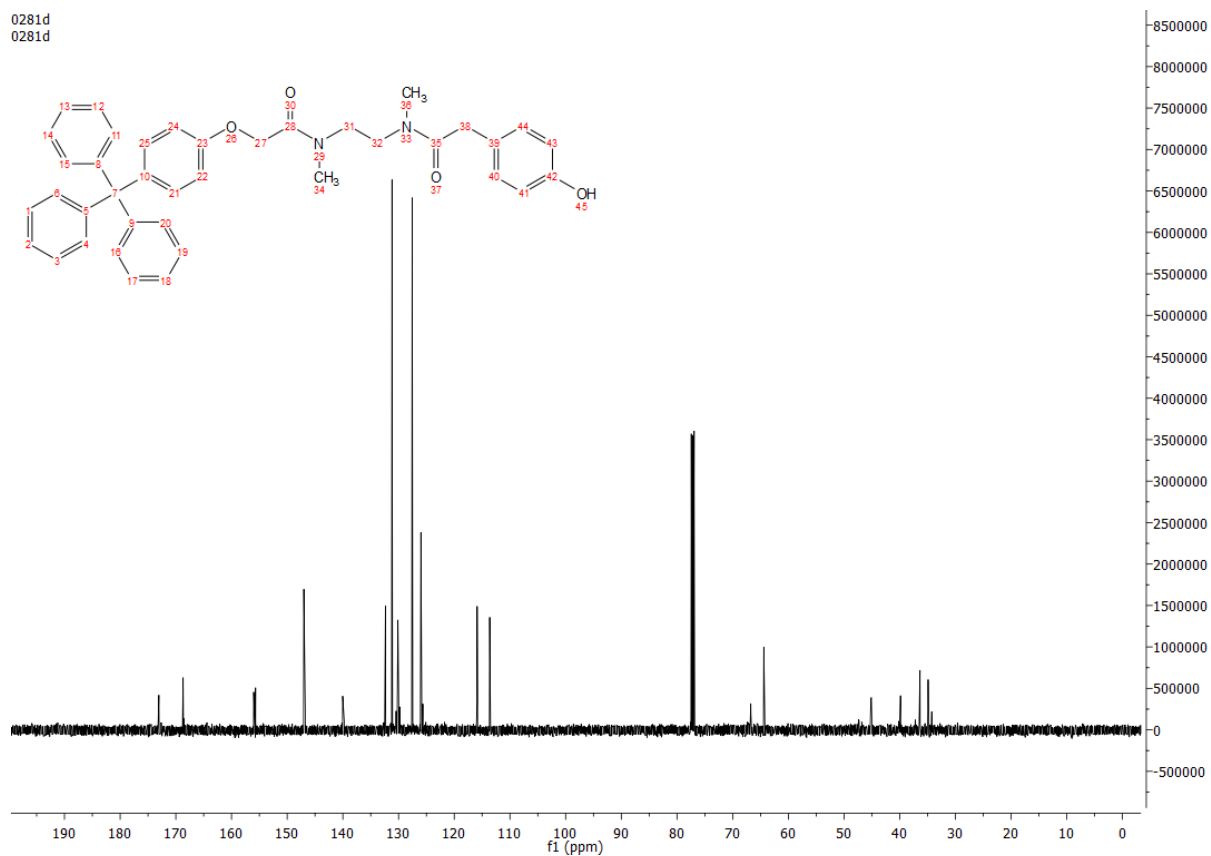
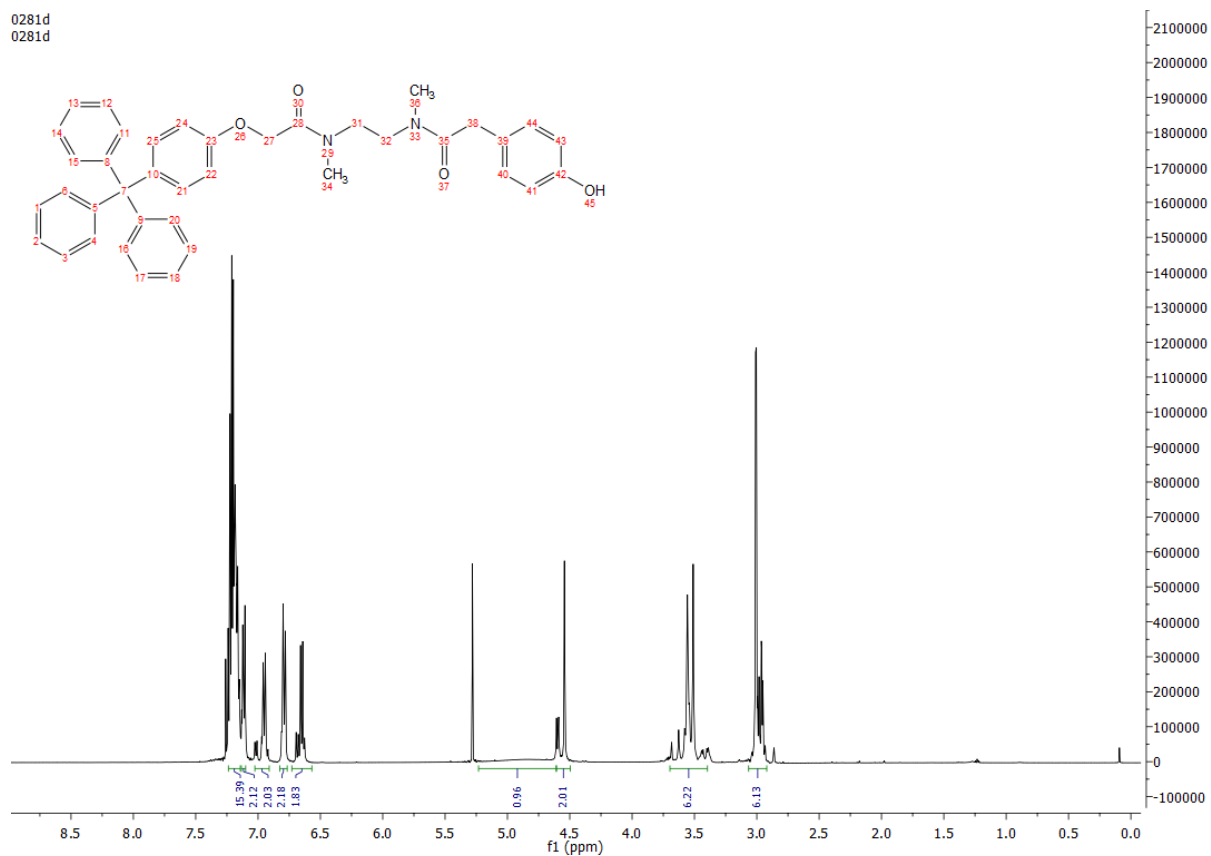


Figure S6: ESI-MS spectrum (DCM, MeOH) of 6.



Sample Name	0281	Position	Vial 1	Instrument Name	Instrument 1	User Name	
Inj Vol	5	InjPosition		SampleType	Sample	IRM Calibration Status	Success
Data Filename	3441_Schwarz_0281.d	ACQ Method		Comment	DCM/MeOH	Acquired Time	7/8/2016 10:22:11 AM

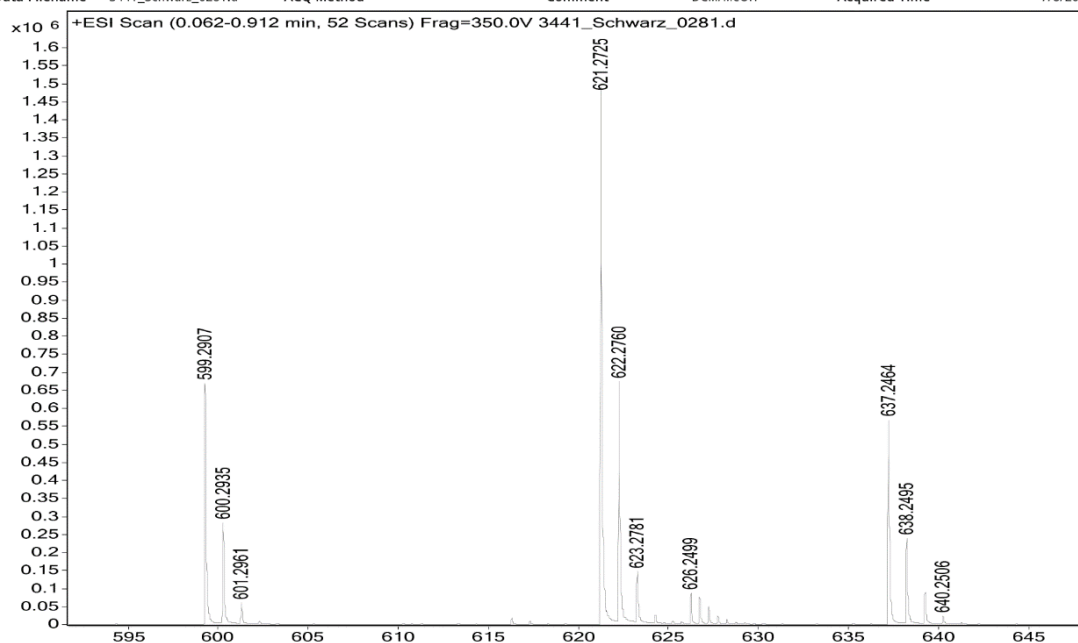


Figure S9: ESI-MS spectrum (DCM, MeOH) of 7.

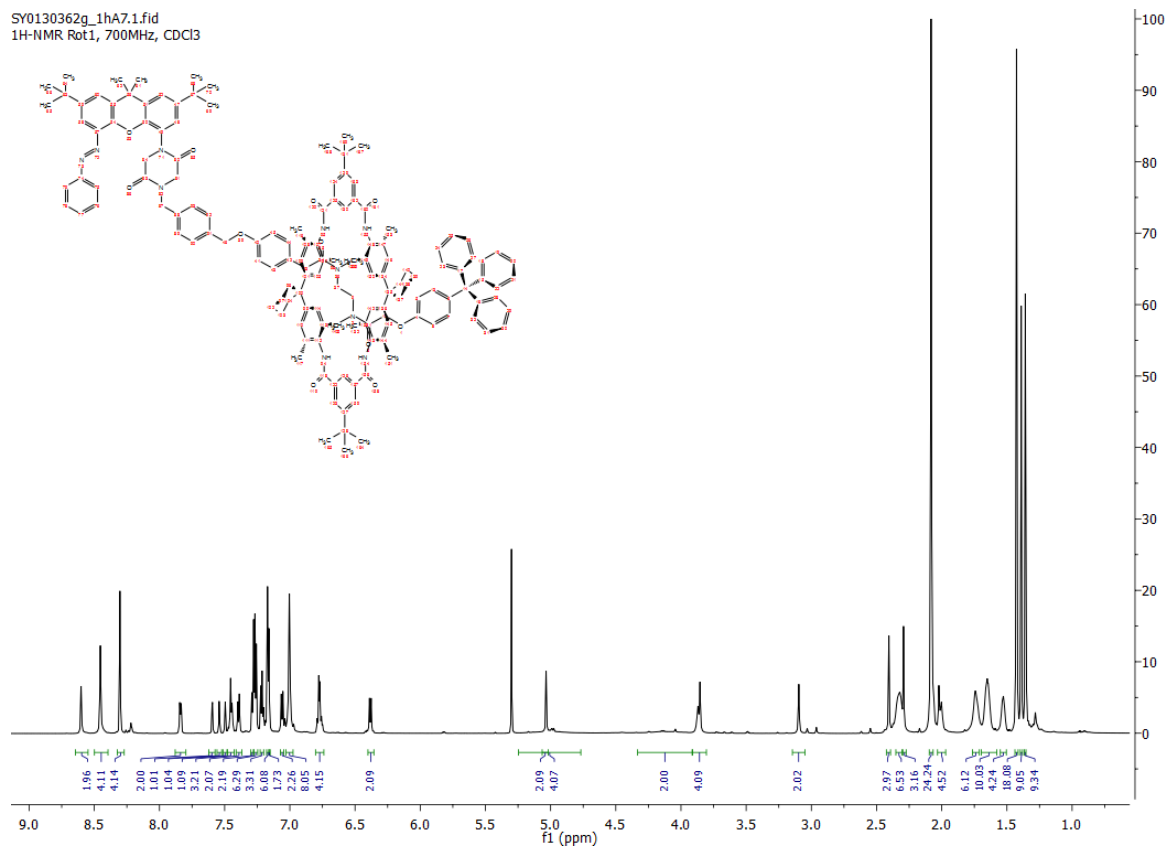


Figure S10: <sup>1</sup>H NMR spectrum (298 K, CDCl<sub>3</sub>) of Rot1.

SY0130362g\_13cA7.1.fid  
13C-NMR Rot1, 176MHz, CDCl3

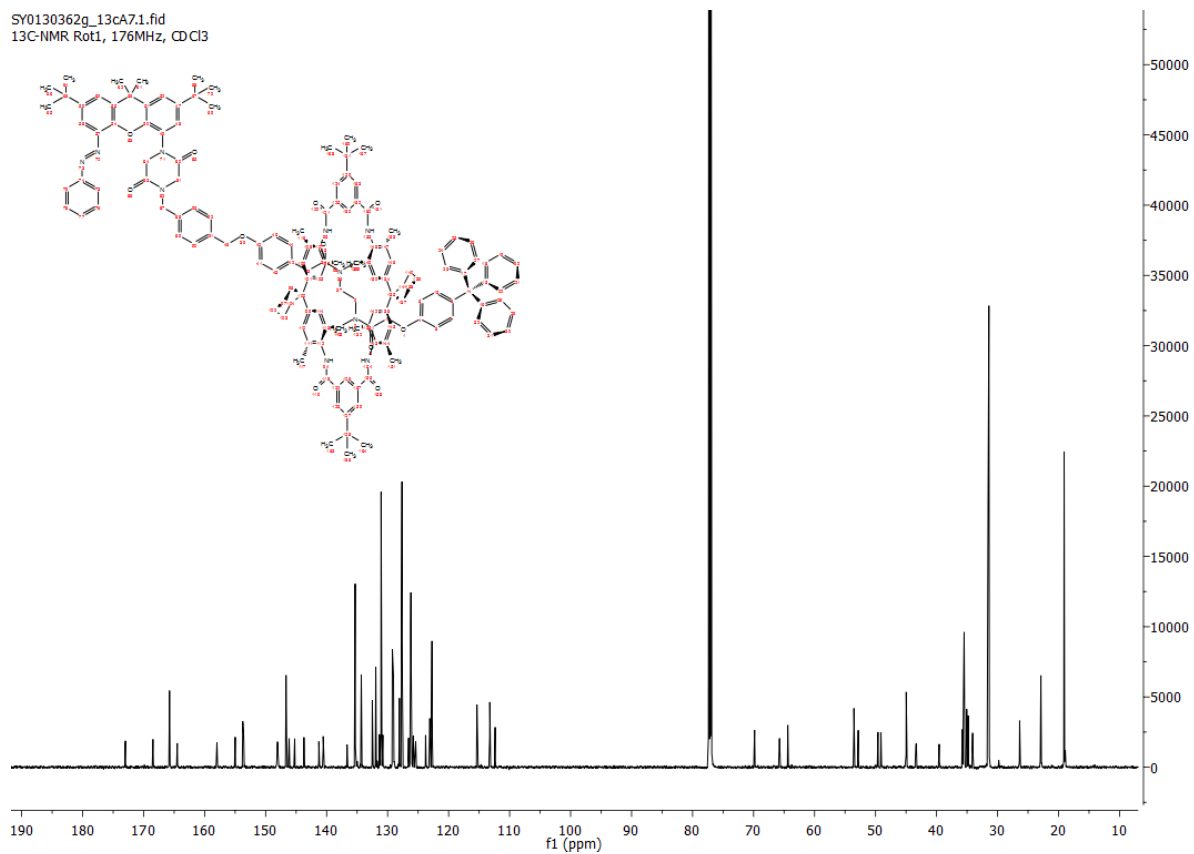


Figure S11: <sup>13</sup>C NMR spectrum (298 K, CDCl<sub>3</sub>) of Rot1.

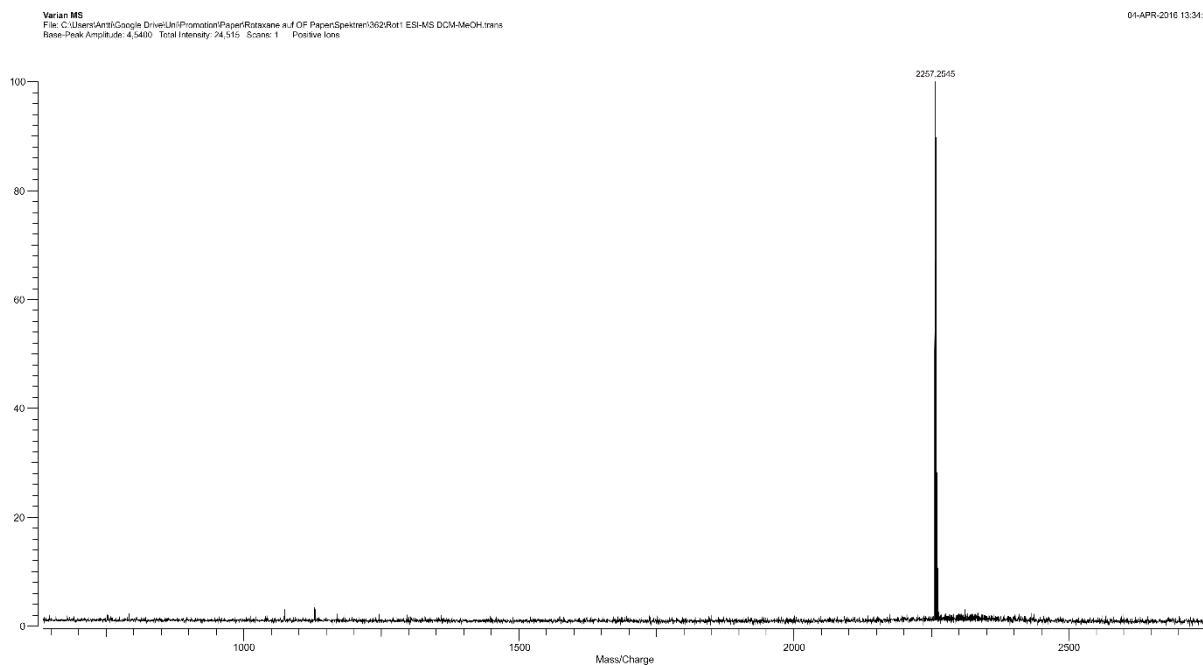


Figure S12: ESI-MS spectrum (DCM, MeOH) of Rot1.

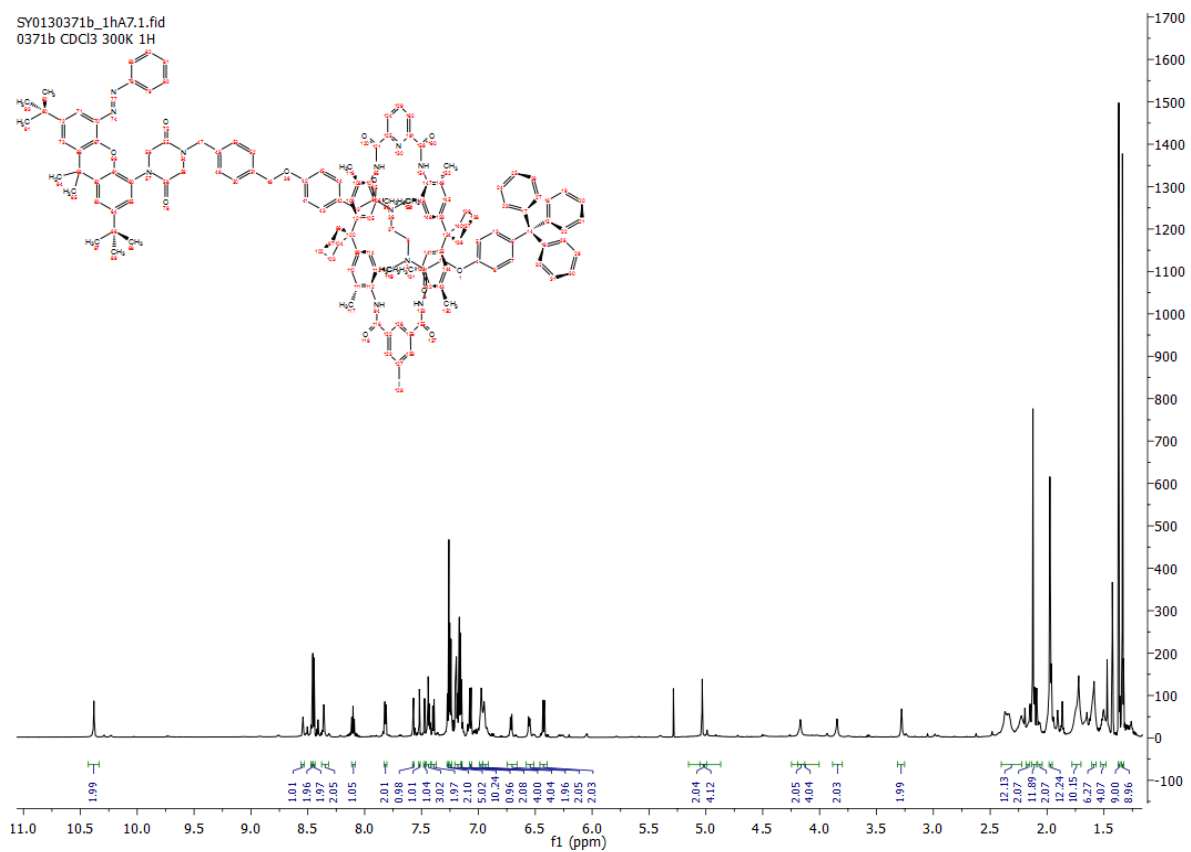


Figure S13:  $^1\text{H}$  NMR spectrum (298 K,  $\text{CDCl}_3$ ) of Rot2.

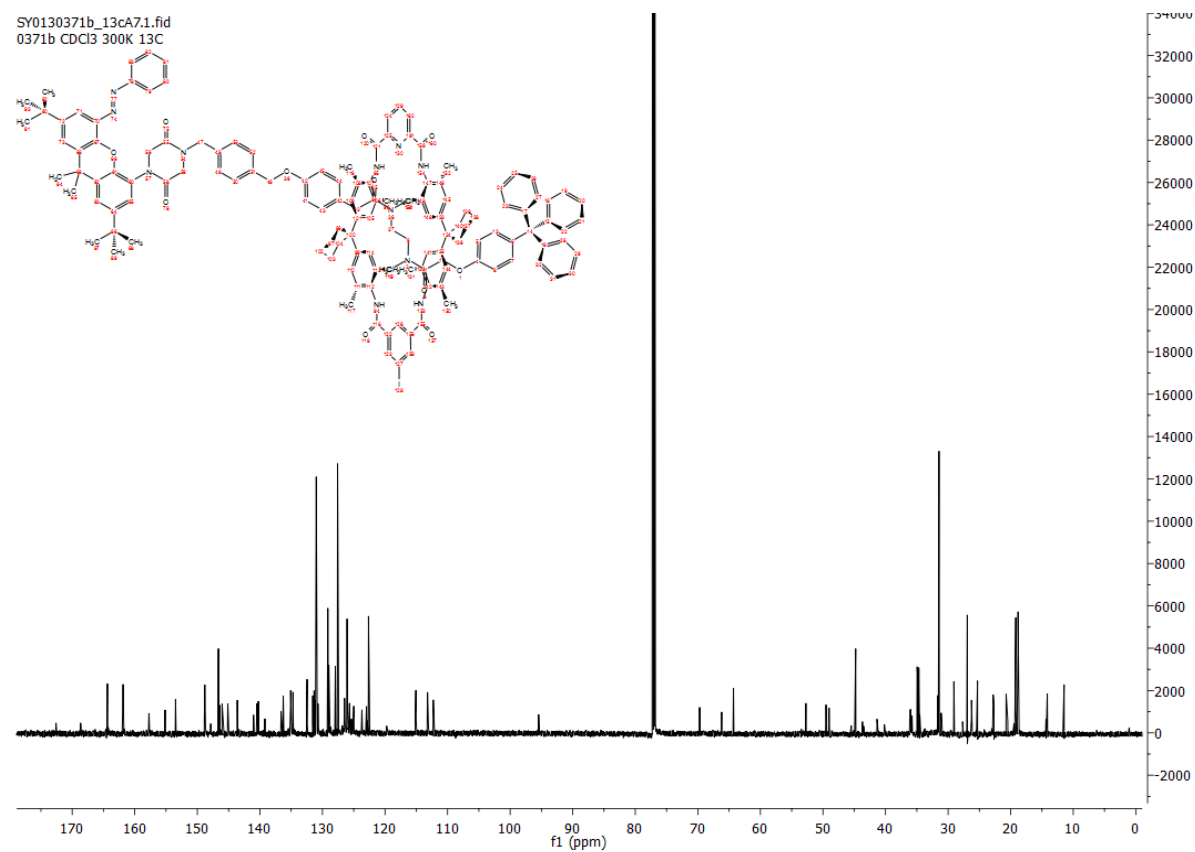


Figure S14:  $^{13}\text{C}$  NMR spectrum (298 K,  $\text{CDCl}_3$ ) of Rot2.

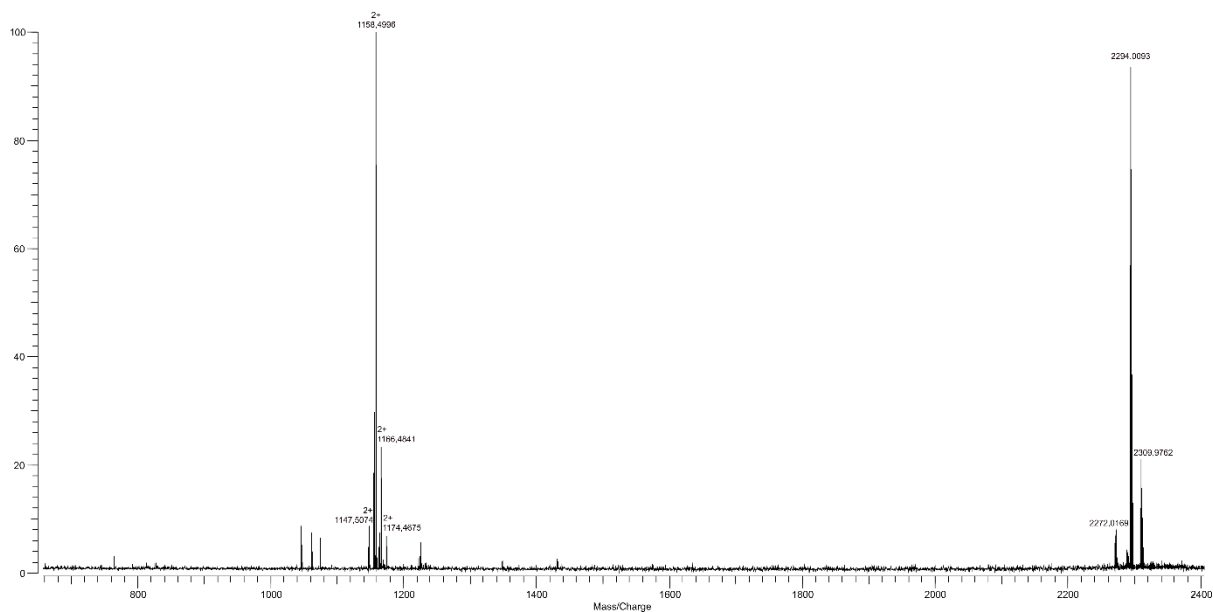


Figure S15: ESI-MS spectrum (DCM, ACN) of Rot2.

SY0130372d\_1hA7.1.fid  
Rot3, <sup>1</sup>H-NMR, CDCl<sub>3</sub>

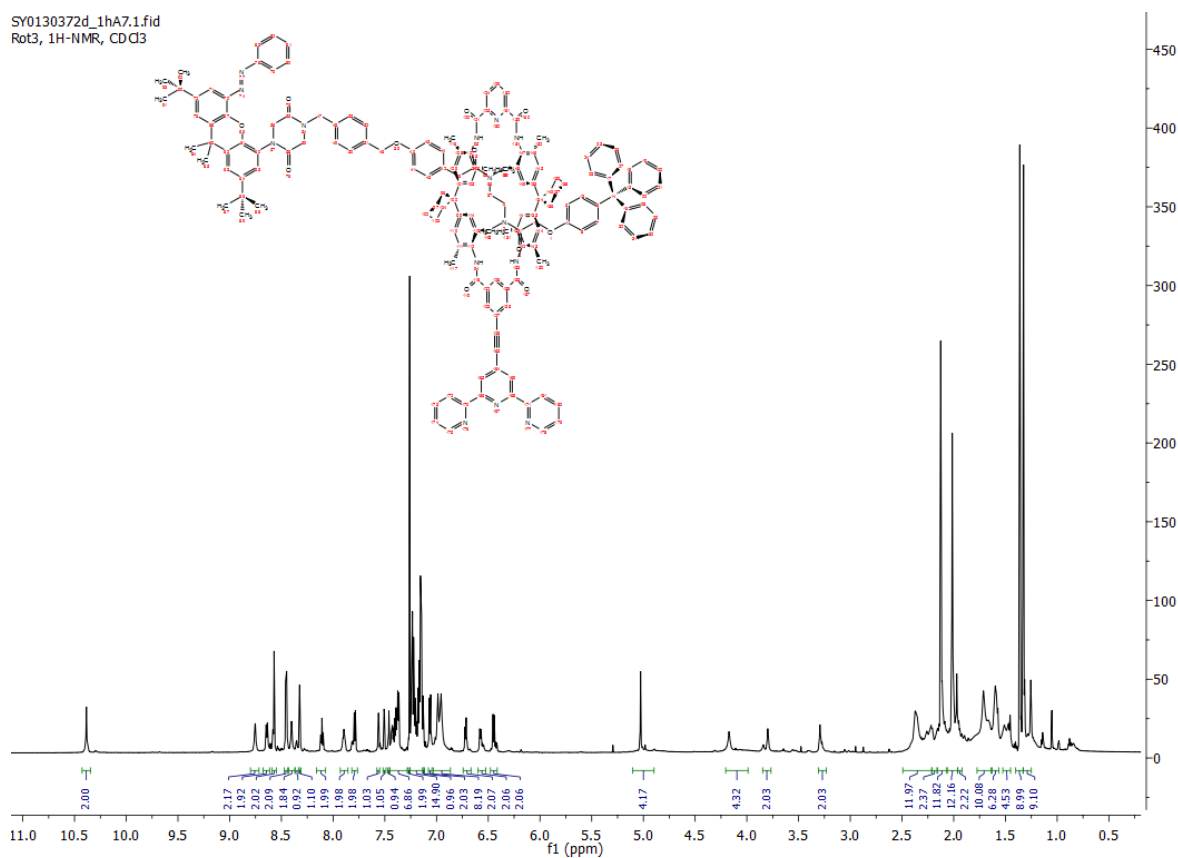


Figure S16: <sup>1</sup>H NMR spectrum (298 K, CDCl<sub>3</sub>) of Rot3.

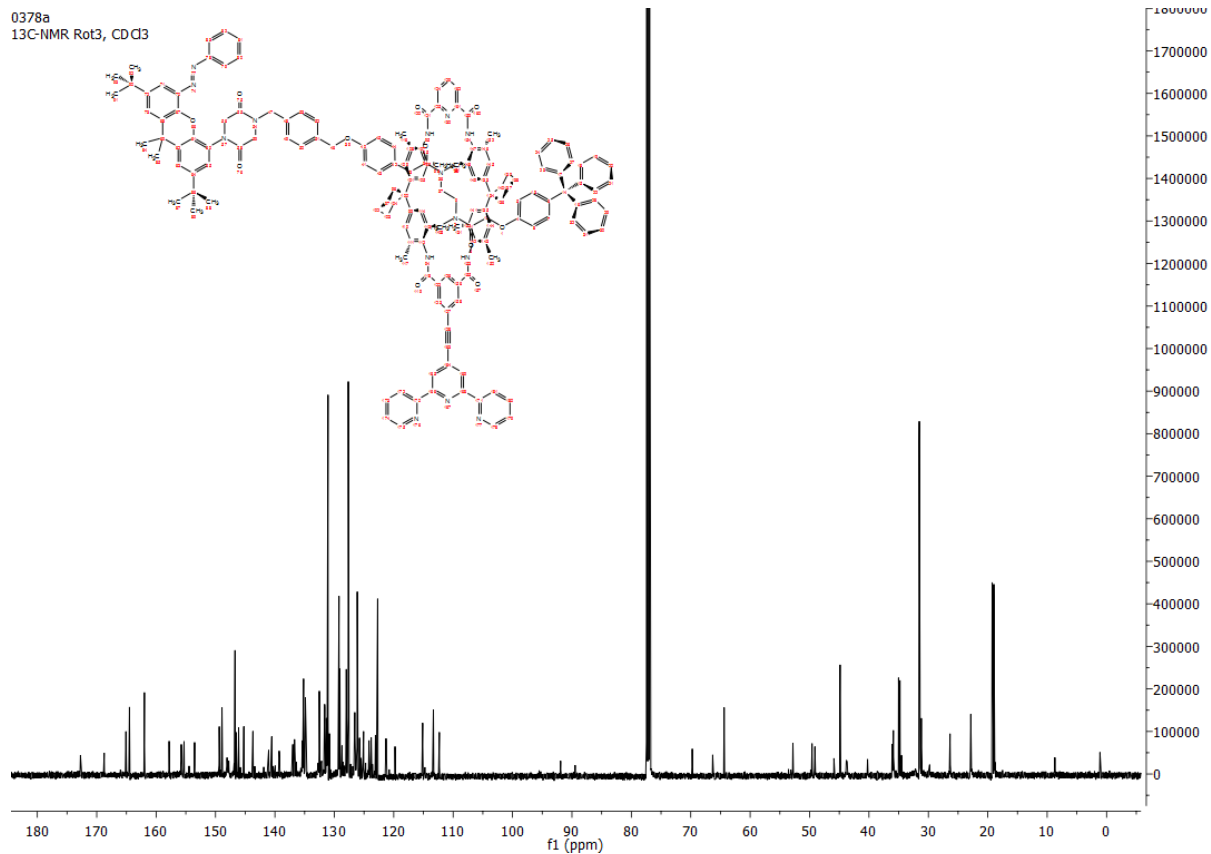


Figure S17: <sup>13</sup>C NMR spectrum (298 K, CDCl<sub>3</sub>) of Rot3.

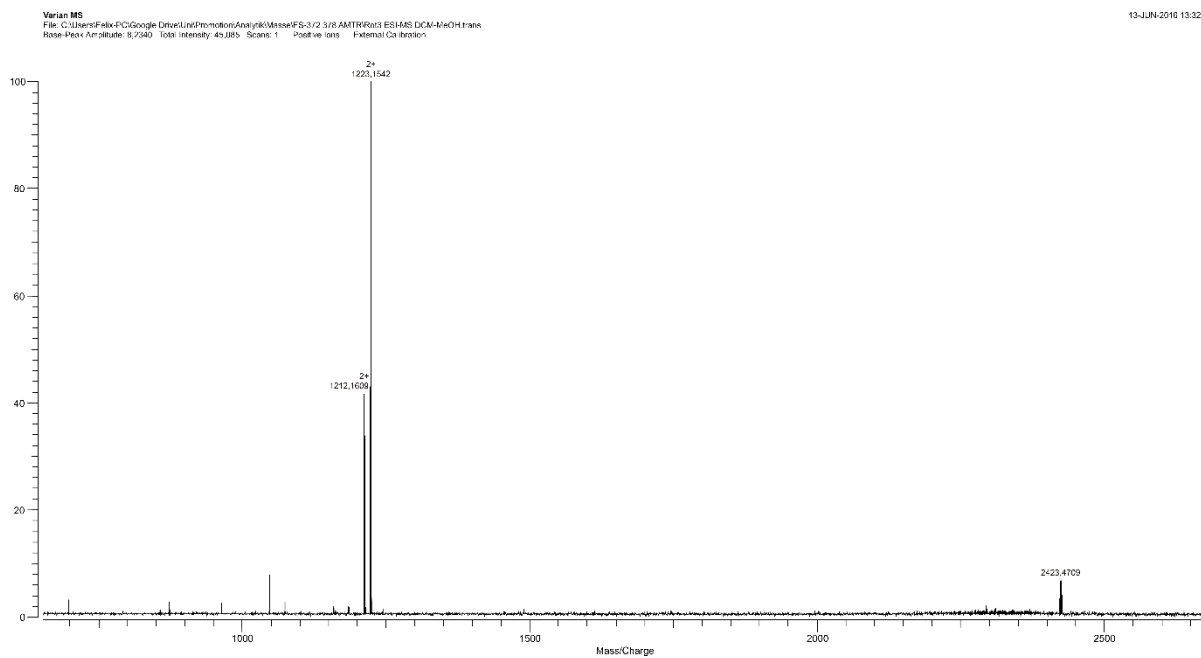


Figure S18: ESI-MS spectrum (DCM, ACN) of Rot3.

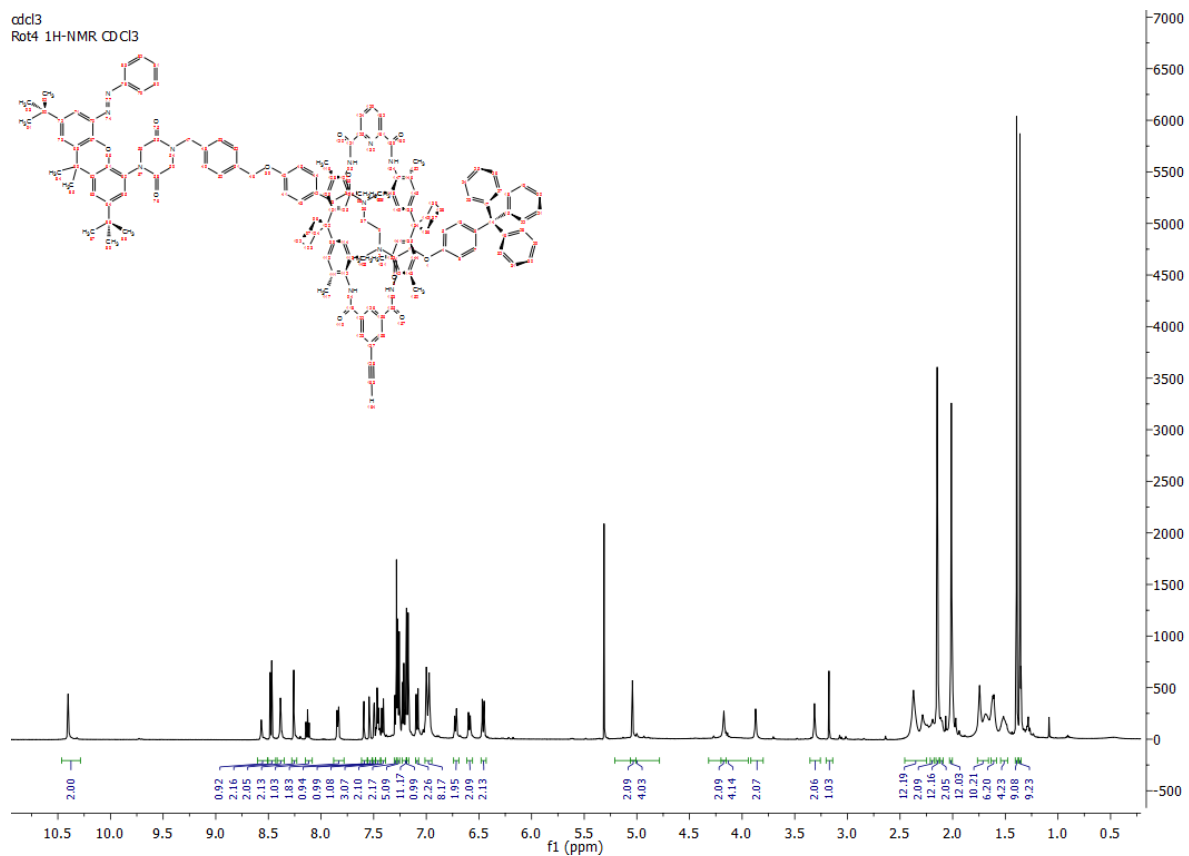


Figure S19:  $^1\text{H}$  NMR spectrum (298 K,  $\text{CDCl}_3$ ) of Rot4.

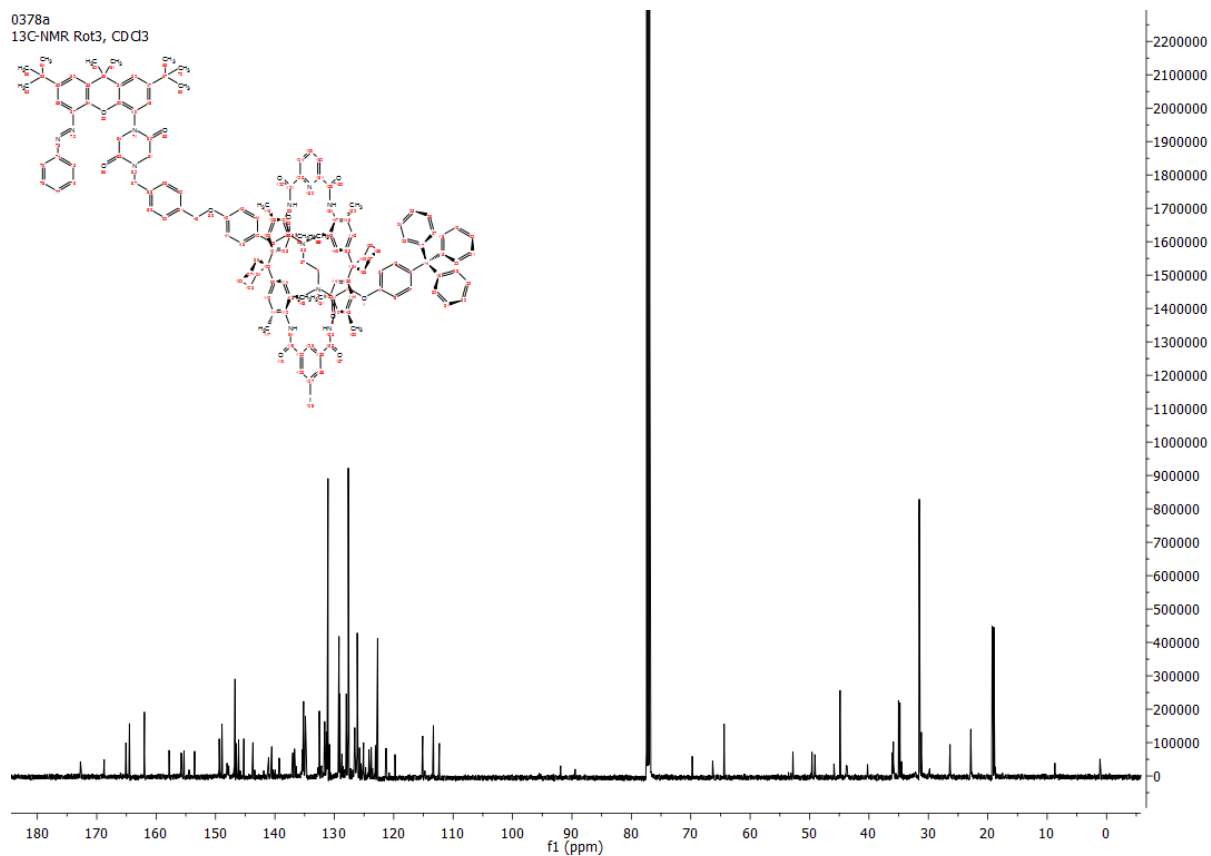


Figure S20:  $^{13}\text{C}$  NMR spectrum (298 K,  $\text{CDCl}_3$ ) of Rot4.

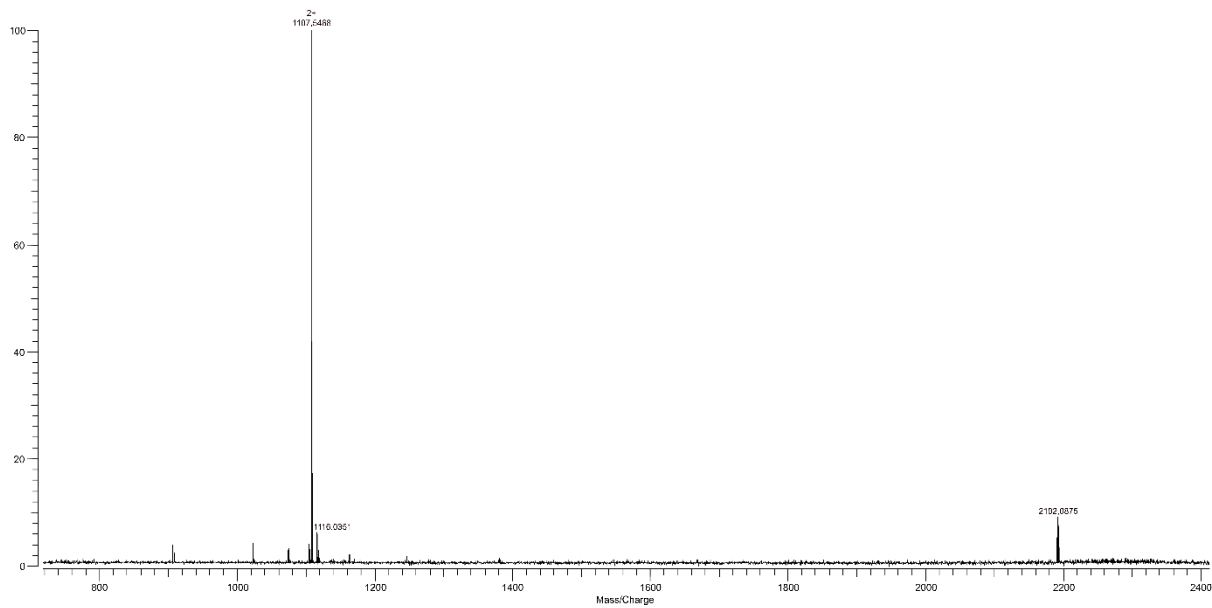
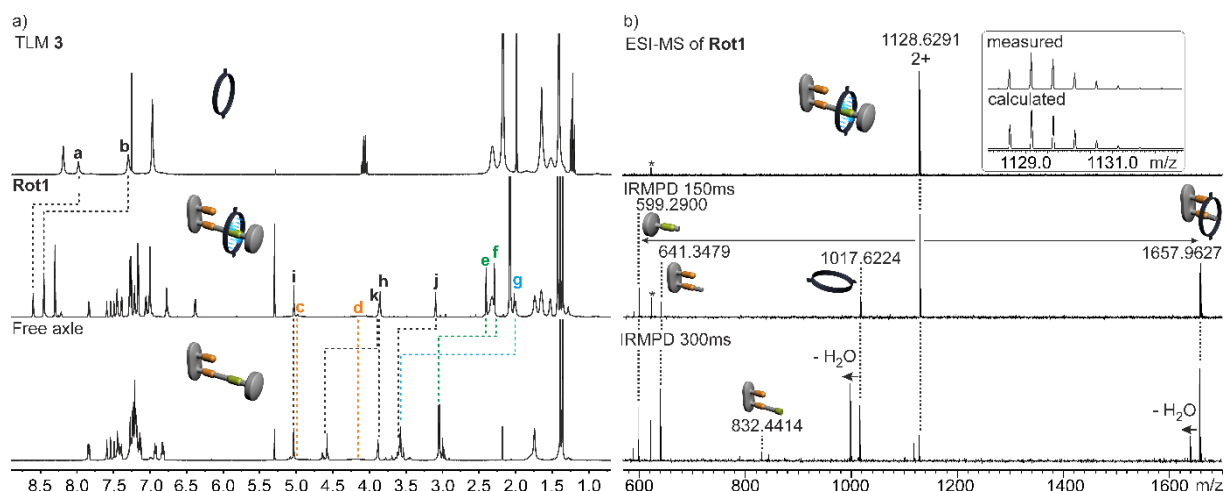


Figure S21: ESI-MS spectrum (DCM, ACN) of Rot4.

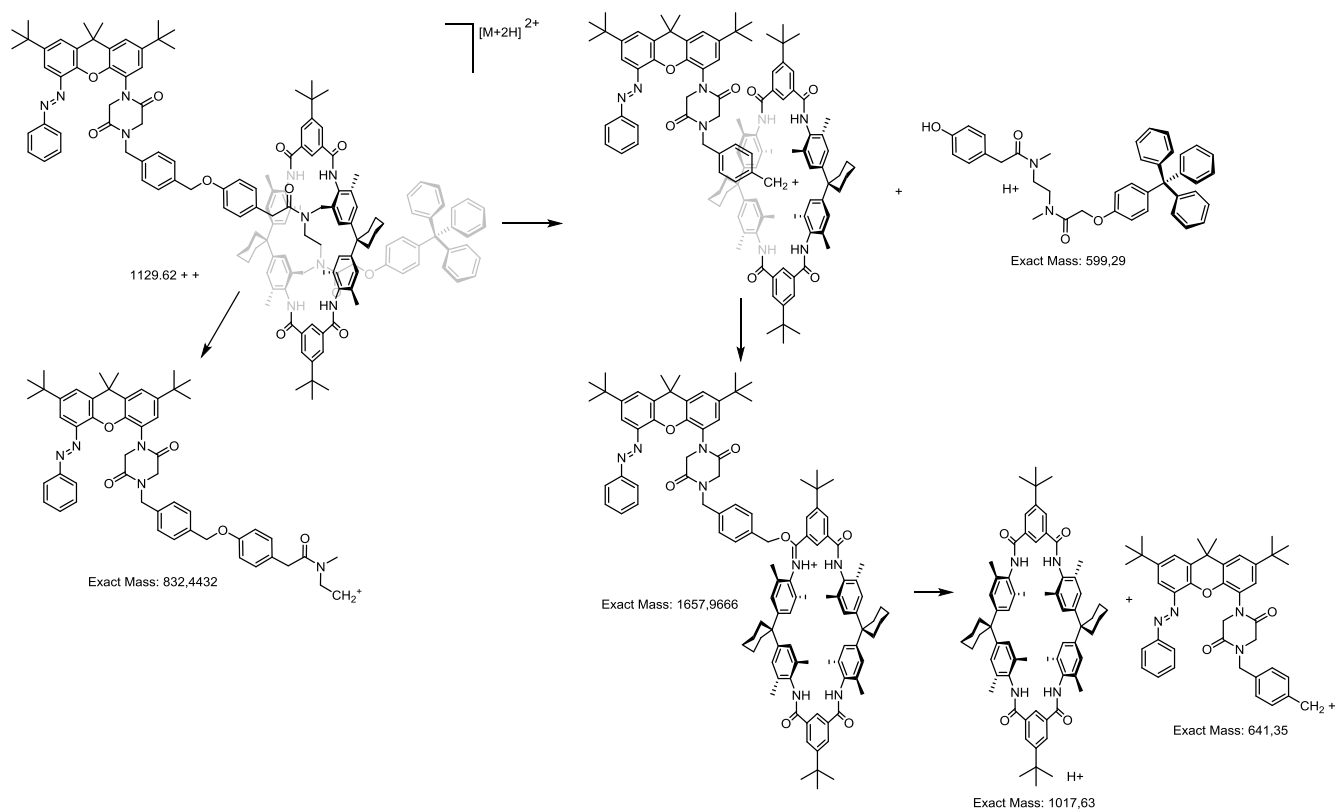
## 5. $^1\text{H}$ NMR and IRMPD-ESI-FTICR MS spectra for the formation of **Rot1**



**Figure S22** a)  $^1\text{H}$  NMR spectra of TLM 3 (top), Rot1 (middle) and the free axle of the rotaxane (down); b) ESI-FTICR MS spectra and IRMPD fragmentation of Rot1.

The formation of **Rot1** was followed by  $^1\text{H}$  NMR spectroscopy (Figure 2d; i, ii). The  $^1\text{H}$  NMR spectrum of TLM **1** shows the macrocycle amide and inner isophthalic protons **a** and **b** at 7.30 respectively 7.98 ppm, which are shifted downfield by 1.15 and 0.62 ppm in the spectrum of the rotaxane due to hydrogen bonding to the axle. Comparison of the NMR spectra of free axle and rotaxane reveals significant upfield shifts of the diamide methyl and methylene protons **e**, **f** and **g** of 0.66, 0.75 and 1.56 ppm and the adjacent methylene protons **j** and **k** of 0.48 and 0.75 ppm due to the shielding effect of TLM **1**, while the methylene protons **c** and **d** of the diketopiperazine binding site remain unaffected at 5.01 and 4.11 ppm. This is clear evidence for the TLM being located at the diamide and not at the diketopiperazine binding site.

The ESI-FTICR MS spectrum shows a peak for the rotaxane dication at  $m/z$  1128, with the isotope pattern being in agreement with the calculated one. IRMPD fragmentation of this ion leads to fragmentation of the axle at the ether bond between the two phenyl rings, yielding two singly charged fragments at  $m/z$  599 and 1658. Fragment 1658 consisting of the macrocycle and part of the axle further dissociates simultaneously. As no separation of axle and macrocycle without the fragmentation of a bond could be observed, it can be concluded that axle and macrocycle are mechanically interlocked.



Scheme S2: Peak assignment for IRMPD spectra of Rot1.

As a control experiment,  $^1\text{H}$  NMR and MS spectra of a 1:1 mixture of the free axle of **Rot1** and TLM **1** have been recorded (Figure S23). The mixture was equilibrated at room temperature over 24h prior to all measurements.

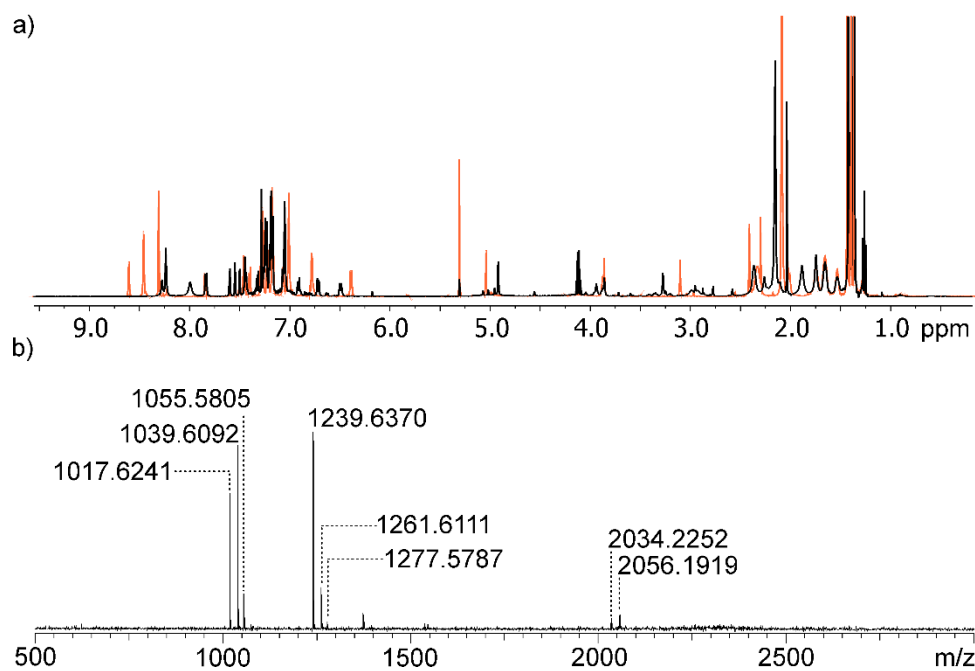


Figure S23: a)  $^1\text{H}$  NMR spectra of Rot1 (orange) and a 1:1 mixture of TLM 1 and the free axle of Rot1 (black) in  $\text{CDCl}_3$  at room temperature and b) ESI-MS spectrum of a 1:1 mixture of TLM 1 and the free axle of Rot1.

The  $^1\text{H}$  NMR spectrum of the 1:1 mixture of TLM **1** and the free axle of **Rot1** (Figure S23a, black) clearly differs from the spectrum of **Rot1** (Figure S23a, orange). The downfield shifts of the macrocycles amide and inner isophthalic protons indicate the formation of side-on complexes. The protons of the diamide binding site are not shifted upfield in the 1:1 mixture, which shows that they are not encapsulated by the macrocycle.

The ESI-MS spectrum (Figure S23b) exhibits signals for the free macrocycle ( $m/z = 1017$   $[\text{M}+\text{H}]^+$ ,  $1039$   $[\text{M}+\text{Na}]^+$ ,  $1055$   $[\text{M}+\text{K}]^+$ ,  $2034$   $[2\text{M}+\text{H}]^+$ ,  $2034$   $[2\text{M}+\text{Na}]^+$ ) and the free axle ( $m/z = 1239$   $[\text{M}+\text{H}]^+$ ,  $1261$   $[\text{M}+\text{Na}]^+$ ,  $1277$   $[\text{M}+\text{K}]^+$ ), while no signals for a 1:1 complex of axle and macrocycle are present. The absence of any side-on complexes is not surprising, as side-on complexes with TLM usually are non-detectable in the gas phase.

Both experiments confirm that in a 1:1 mixture of free axle and macrocycle, the macrocycle does not thread the axle.

## 6. Variable-temperature $^1\text{H}$ NMR spectra of **Rot1**

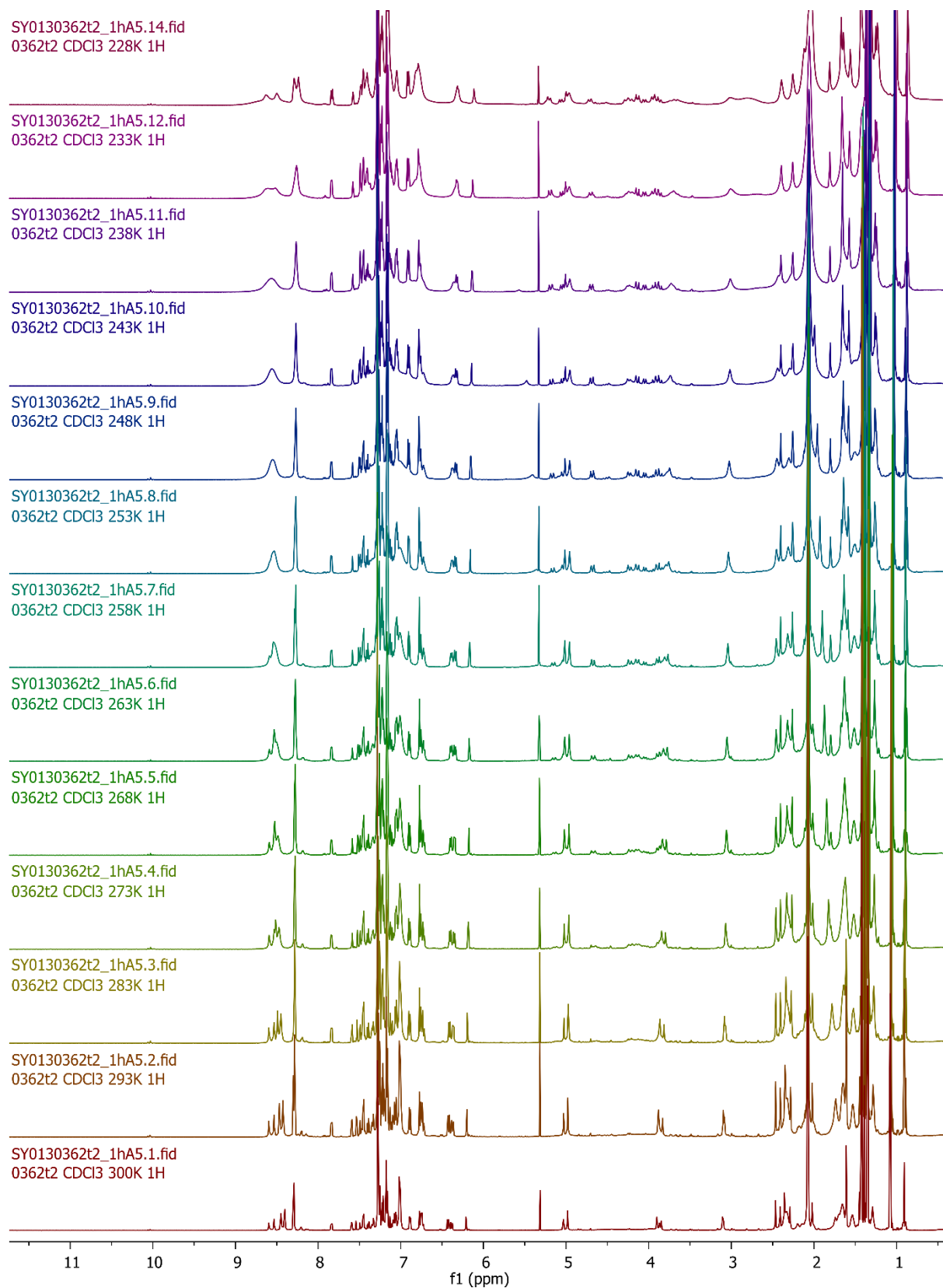


Figure S24: Variable temperature 500 MHz  $^1\text{H}$  NMR spectra of Rot1 in  $\text{CDCl}_3$  from 300 K to 228 K.

## 7. Determination of binding constants

The binding behaviour of diamide **7** to TLM **1** was investigated with NMR experiments. Since there is a fast exchange on the NMR timescale, the binding constants were evaluated by NMR titration analysis.<sup>8,9</sup> A solution of TLM **1** (5.00 mg) in CDCl<sub>3</sub> (0.65 mL) was placed in an NMR tube and treated with different amounts of **2**. A <sup>1</sup>H NMR spectrum was measured after each injection and the guest concentrations were determined by integration of the signals. The binding constant was determined based on a 1:1 binding model to be 1,400 ± 140 M<sup>-1</sup>.

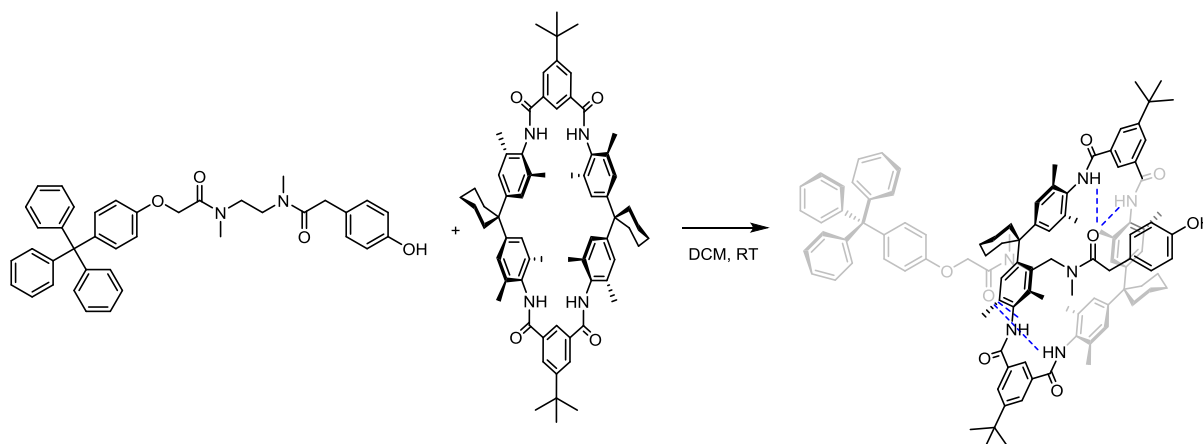


Figure S25: Pseudorotaxane formation.

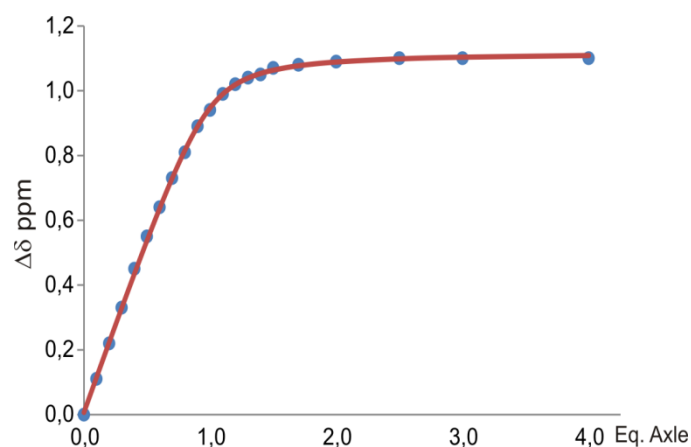


Figure S26: NMR titration.

## 9. Clicked surfaces

To deposit **Rot4**, glass surfaces were functionalized with a self-assembled monolayer of **AUS** ((11-azidoundecyl)triethoxysilane) by immersing the substrate in a 5 mM solution of **AUS**. Immersing these surfaces in a 1 mM solution of **Rot4** in the presence of a catalytic amount of **Cat**, **Rot4** was covalently attached to the SAM in an azide-alkyne click-reaction (Figure S27a). On-surface switching was conducted likewise to the surfaces functionalized with **Rot3** and resulted in the same effects (Figure S27b).

The surfaces functionalized with **Rot4** were analysed with transmission UV-Vis spectroscopy analogously to the surfaces with **Rot3**. An increase in absorbance was detected in the UV-Vis spectrum after deposition of **Rot4**, which resembles to the UV-Vis spectra of **Rot1** in solution and therefore indicates a successful monolayer formation. After irradiation at  $\lambda_1 = 365$  nm, the UV-Vis

spectra of the surface showed a decrease in absorbance in the region between 300 and 500 nm, indicating the formation of *cis*-configured **Rot4**. After irradiation at  $\lambda_2 = 470$  nm, the absorbance of the surface increased up to about 90 % of its initial value, indicating almost complete back-switching to the *trans*-configuration of **Rot4** (Figure S27, c).

The stronger absorbance for the surfaces functionalized with **Rot3** in comparison to the surfaces with **Rot4** leads to the conclusion that a larger amount of **Rot3** than **Rot4** was deposited and thus the monolayer is packed more densely. XPS measurements show a molecular ratio of **Rot4** to **AUS** of 1:45, which is about three times lower than the packing density of **Rot3**.

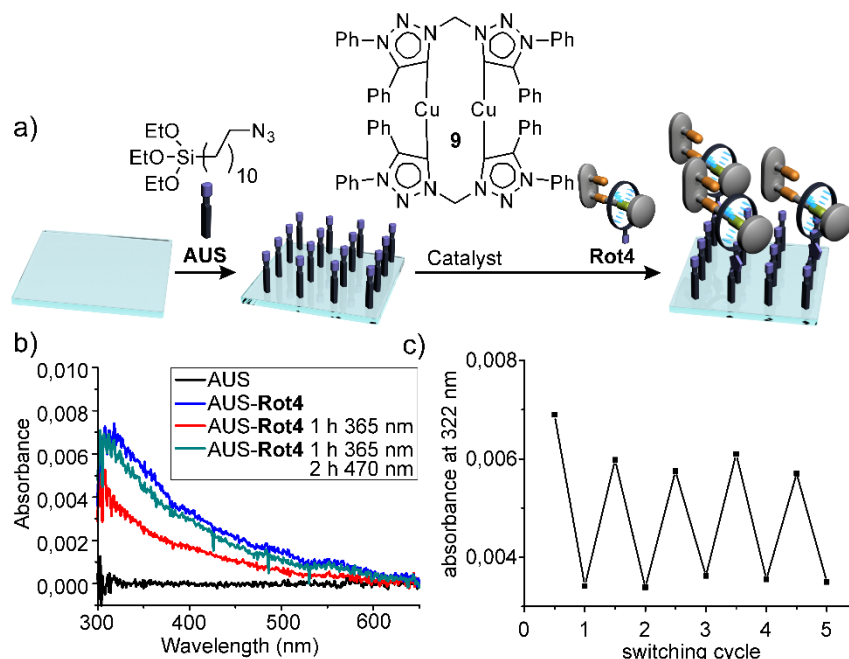


**Figure S27:** a) Surface deposition of **Rot4**, b) transmission UV-Vis spectra of surfaces, c) reversibility of the on-surface photoswitching tested over five cycles.

## 10. Surface preparations

The surface preparation procedures were developed in previous studies of our group. In here, only a simple work instruction without further explanations is given.<sup>10-15</sup>

### Surface cleaning

Glass slides and silicon wafers were cut to 2cm<sup>2</sup> size and cleaned by immersing them for 30 min in piranha solution (H<sub>2</sub>O<sub>2</sub> 30% : conc. H<sub>2</sub>SO<sub>4</sub> 1:3). The surfaces were then rinsed with dest. water for 1 min.

### Deposition of **Rot3**

Cleaned surfaces were dipped in EtOH to remove the remaining water droplets on the surface, then dipped two times in DCM and then immersed in a 5 mM solution of **PDS** ((12-(4-pyridyl)dodecyl)triethoxysilane) in DCM for 24 h. The surfaces were then dipped two times in DCM followed by immersion in DCM for 10 min to remove any unspecific bound molecules. The surfaces were then dried with an argon stream to record background UV spectra.

The surfaces were immersed in a 1 mM solution of Pd(CH<sub>3</sub>CN)<sub>4</sub>(BF<sub>4</sub>)<sub>2</sub> in acetonitrile for 30 min, then dipped two times in acetonitrile followed by immersion in acetonitrile for 10 min, and then two times in DCM followed by immersion in a 1 mM solution of **Rot3** in DCM for 24 h. Afterwards, the surfaces were dipped two times in DCM, immersed in DCM for 10 min, and dried with an argon stream. The

solvents used for washing the substrates by dipping or immersing were changed after each surface contact.

### Deposition of Rot4

Cleaned surfaces were dipped in EtOH to remove remaining water, subsequently washed two times with toluene and immersed in a 5 mM solution of **AUS** in toluene at 80 °C for 24 h. Followed by rinsing in toluene, twice in DCM and subsequent immersion for 10 min in DCM. The surfaces were then dried with an argon stream to record background UV spectra.

The surfaces were afterwards immersed in a 1 mM solution of **Rot4** containing 5 mol% catalyst **9** for 24 h, then dipped two times in DCM followed by immersion in DCM for 10 min and dried under an argon stream.

## 11. NEXAFS and XPS

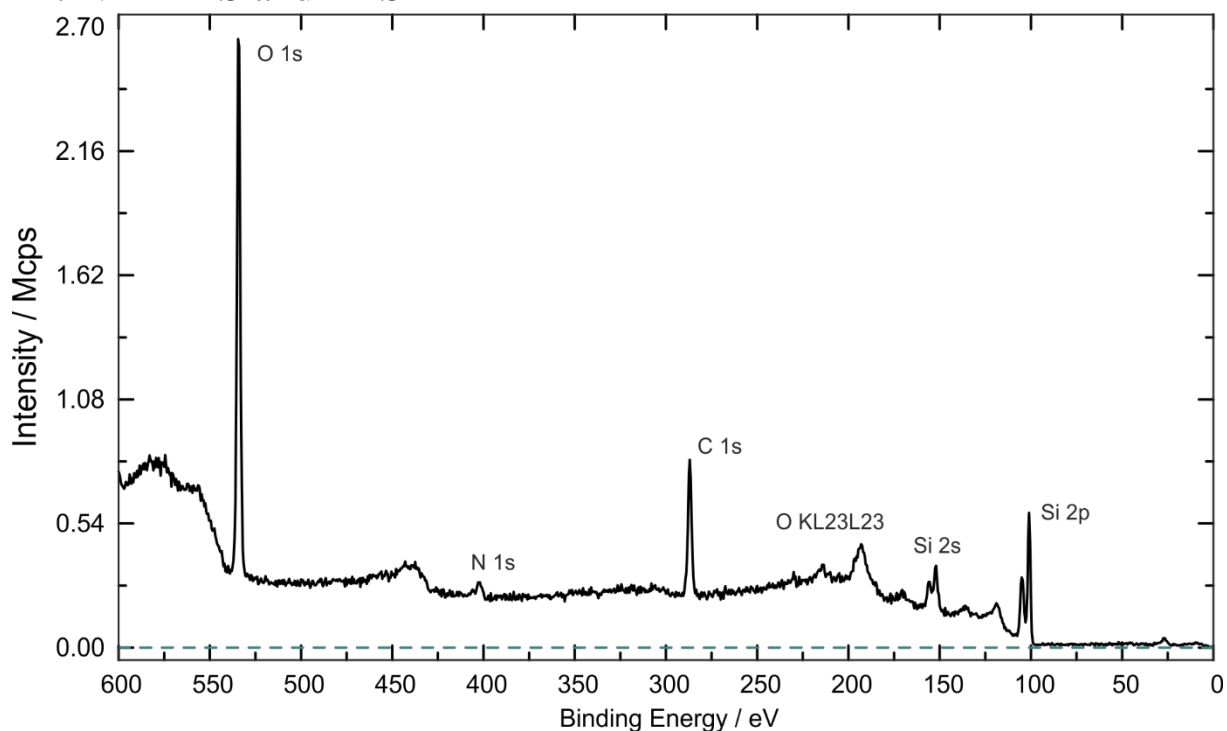


Figure S28. Survey XP-spectrum ( $h\nu = 849$  eV) of the AUS monolayer.

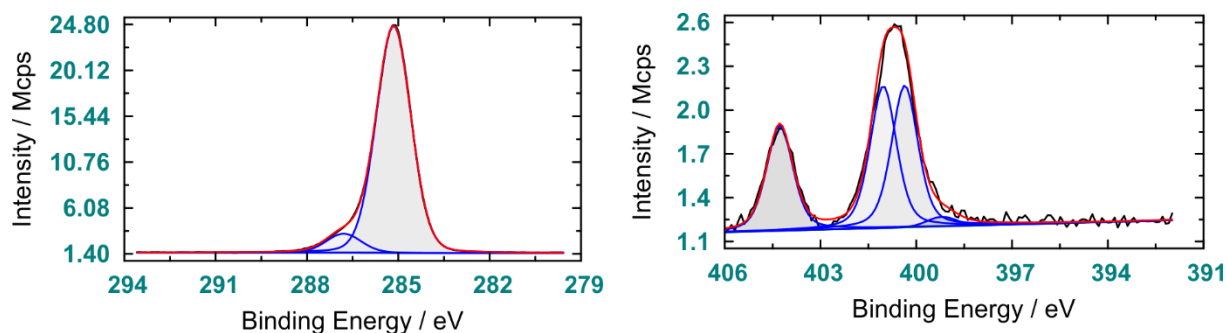


Figure S29. C 1s ( $h\nu = 385$  eV) and N 1s ( $h\nu = 500$  eV) Xp-spectra of the AUS monolayer. Chemical shifts are in line with literature.<sup>16</sup>

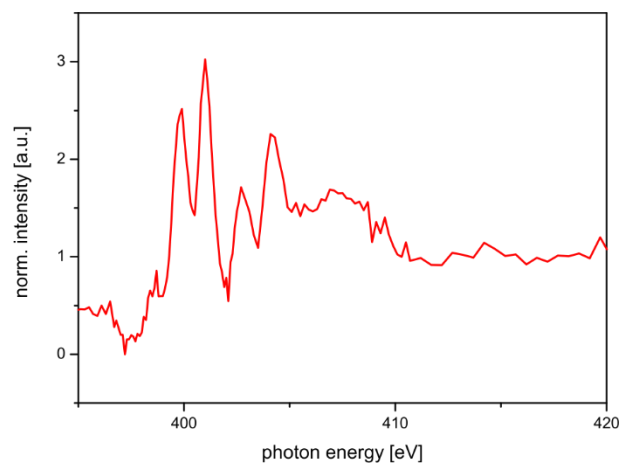


Figure S30. N K-edge NEXAFS spectrum of the AUS monolayer.

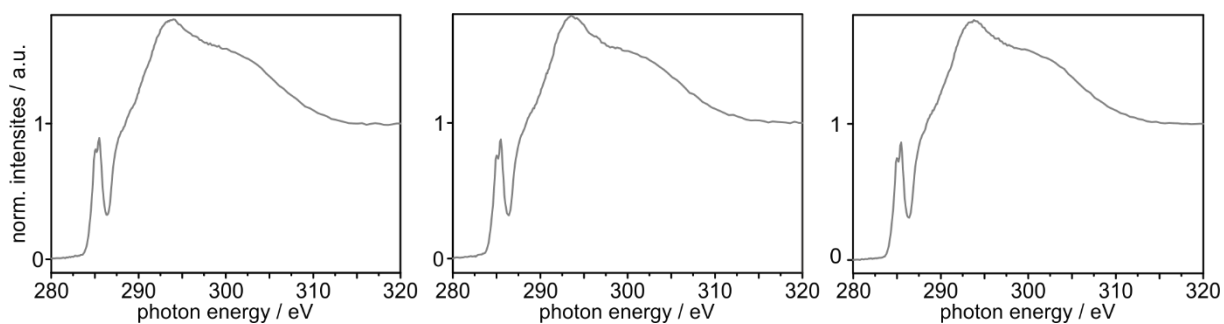


Figure S31: (angle-resolved) C-K NEXAFS spectra of a Rot3-monolayer deposited to Pd-PDS; pristine (left), after irradiation with 365 nm for 1 h (middle), and after 1 h irradiation with 365 nm plus 1.5 h with 470 nm (right).

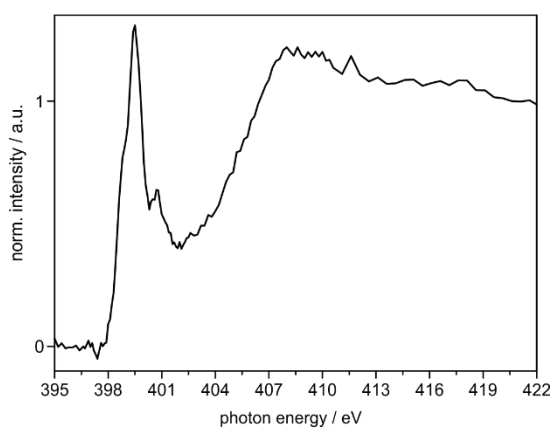


Figure S32: N K-edge NEXAFS spectrum of a Rot3-monolayer deposited to PDS-Pd (PDS-PdRot3).

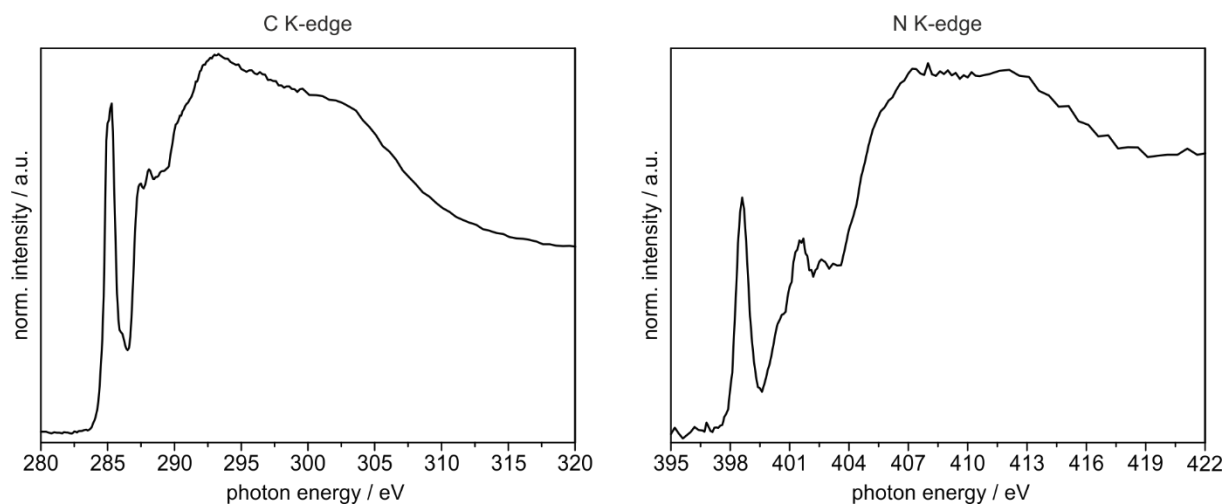


Figure S33: C K-edge (left) and N K-edge (right) of drop-coated Rot3.

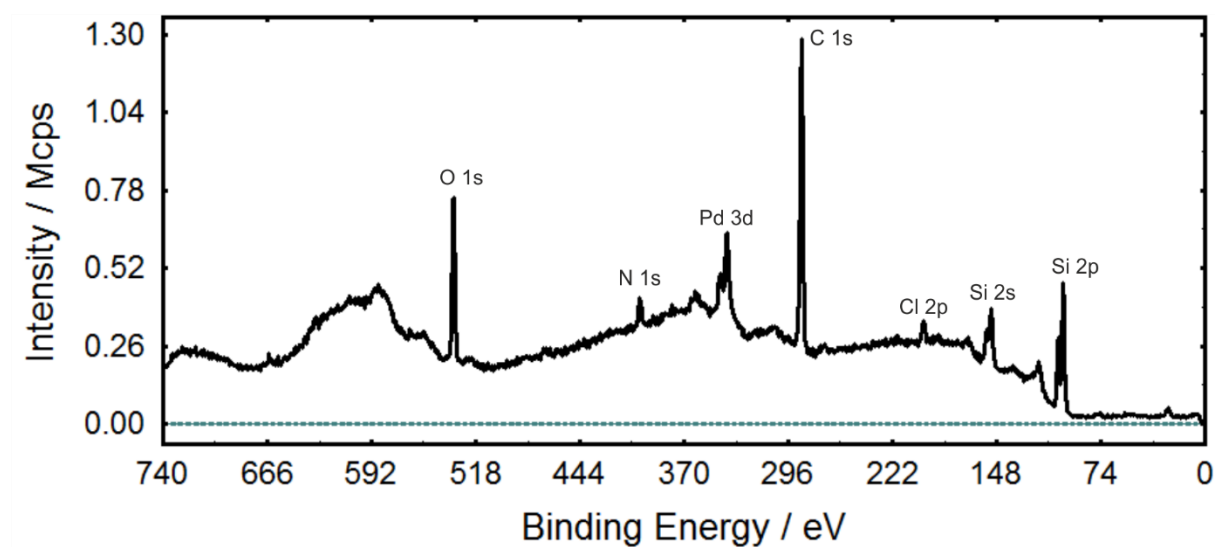


Figure S34: Survey SR-XP spectrum of PDS-PdRot3.

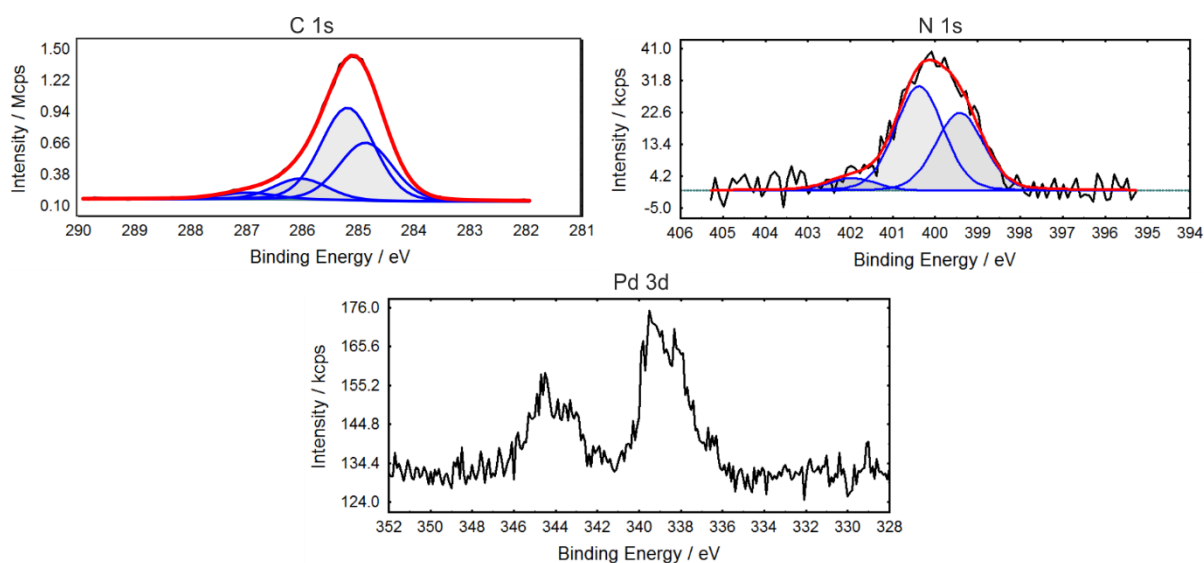


Figure S35: C 1s, N 1s, and Pd 3d SR-XP spectra of PDS-PdRot3.

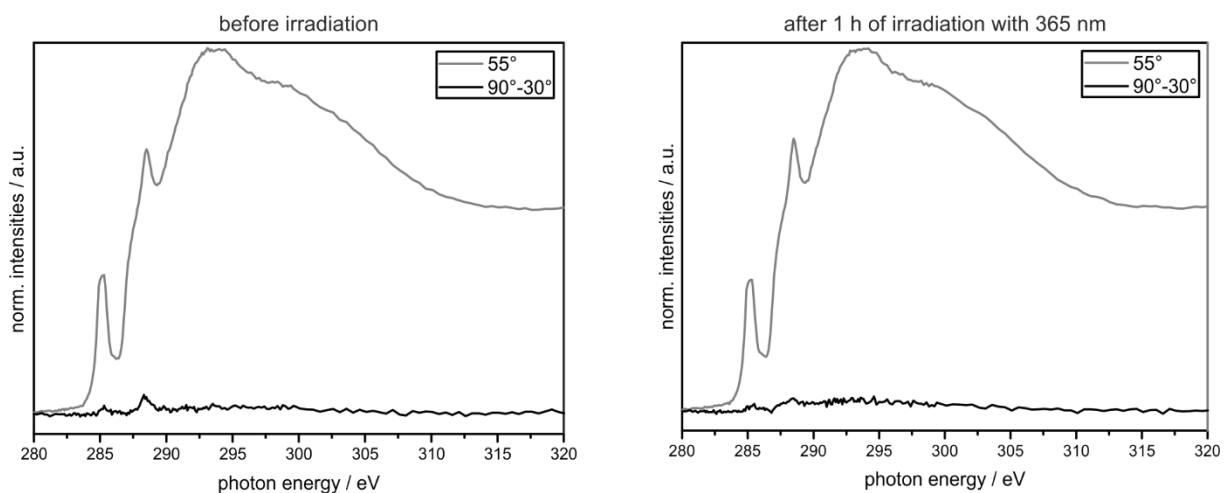


Figure S36: (angle-resolved) C K-edge NEXAFS spectra of Rot4 clicked to AUS (AUS-Rot4).

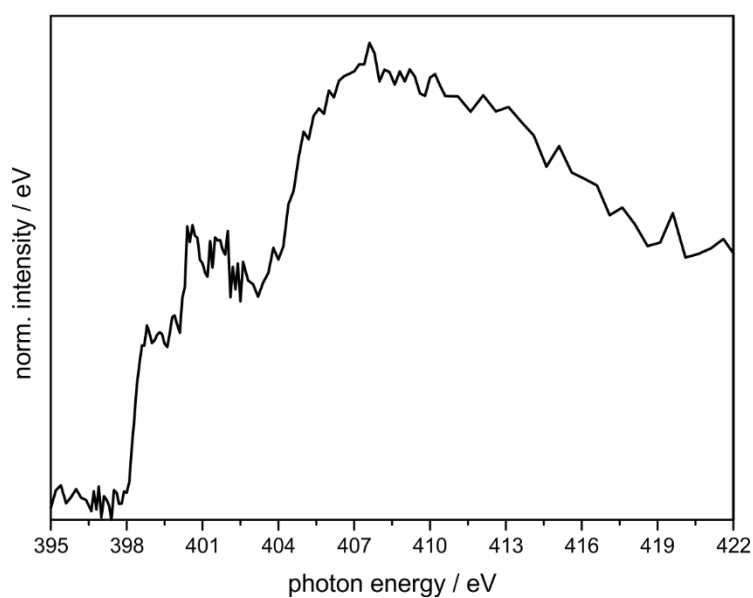


Figure S37: N K-edge NEXAFS of AUS-Rot4.

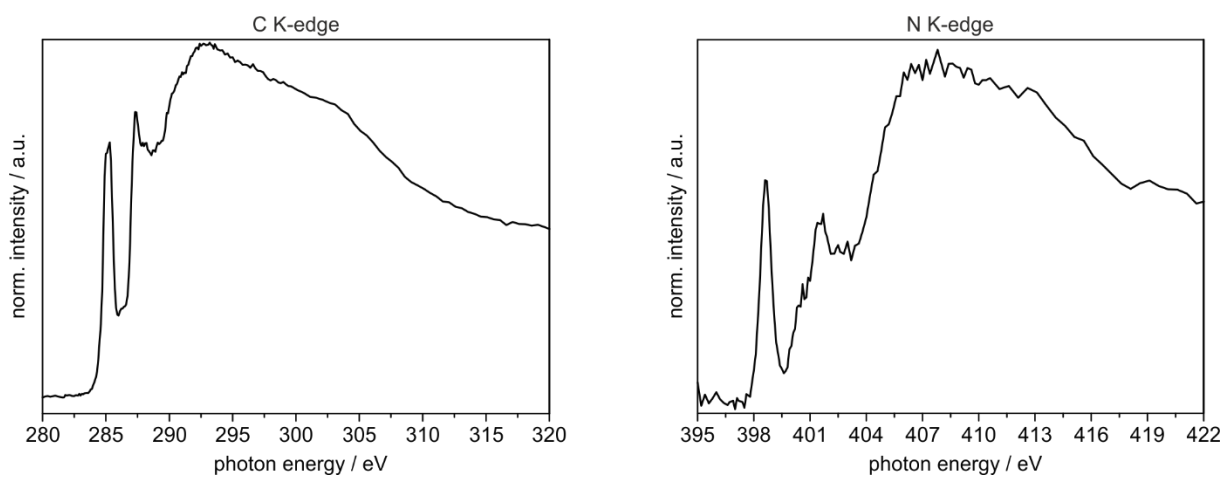


Figure S38: C K-edge (left) and N K-edge (right) NEXAFS spectra of drop-coated Rot4.

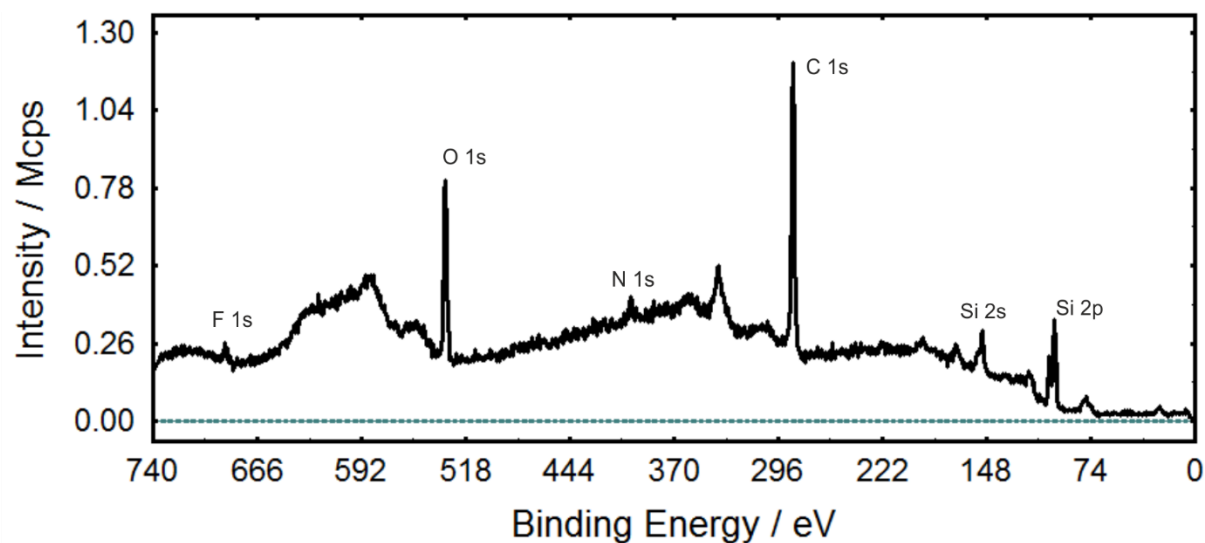


Figure S39: Survey SR-XP spectrum of AUD-Rot4.

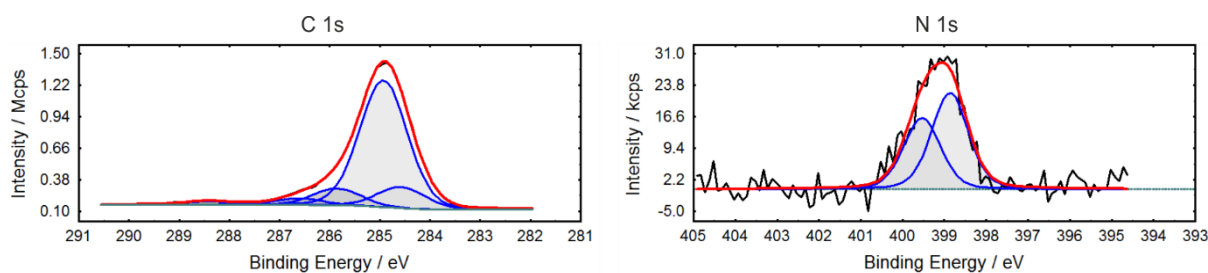


Figure S40: C 1s and N 1s SR-XP spectra of AUD-Rot4.

Table 1. Summary of the C 1s peak fits. Theoretical peak areas for aromatic and aliphatic carbon atoms were calculated for different ratios of the rotaxane to the underlying monolayer. The best fit was obtained at a 1:15 ratio for Rot3 and a 1:45 ratio for Rot 4.

binding energy [eV]	assigned atom	Rot3-PdPDS		Rot4-AUS	
		theor. Value (calc. for 1:15)	rel. peak area (exp.)	theor. Value (calc. for 1:45)	rel. peak area (exp.)
284.7	C <sub>sp2</sub>	32	32	12	12
285.1	-CH <sub>2</sub> -	50	52	70	73
286	CH <sub>2</sub> -N, C <sub>sp2</sub> -N	15	12	15	10
287	CNO	3	4	3	5

## 12. Contact angle measurements

Contact angle measurements were conducted for a **PDS-Rot3** monolayer on a glass surface over five consecutive switching cycles (Figure S37). In each switching cycle, the monolayer was irradiated at  $\lambda_1 = 365$  nm for 1 h and subsequently at  $\lambda_2 = 470$  nm for 1.5 h. The experiments were repeated for every measurement point on two surfaces with three measurement spots on each surface. Averaged values of all measurements are reported. An error of  $1^\circ$  for inaccurate reading, differences in volume of the droplet and the measurement time is assumed. The contact angles display a strong and reversible change in polarity upon photoswitching of the rotaxane monolayer.

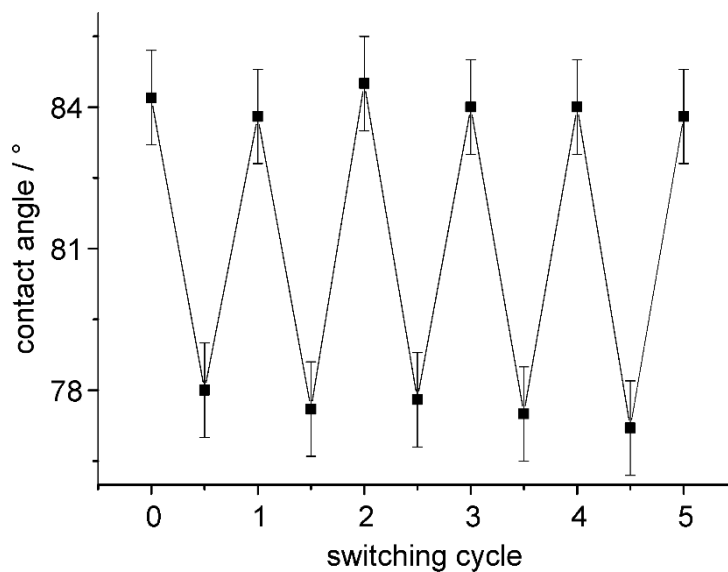


Figure S41: Contact angle measurements.

## 13. References

1. ISO15472:2010, *Journal*, 2010.
2. J. Stöhr, *NEXAFS spectroscopy*, Springer, Berlin, 1992.
3. P. E. Batson, *Phys. Rev. Lett.*, 1982, **49**, 936-940.
4. F. B. Schwarz, T. Heinrich, J. O. Kaufmann, A. Lippitz, R. Puttreddy, K. Rissanen, W. E. S. Unger and C. A. Schalley, *Chem. Eur. J.*, 2016, **22**, 14383-14389.
5. V. Grosshenny, F. M. Romero and R. Ziessel, *J. Org. Chem.*, 1997, **62**, 1491-1500.
6. W. Zhou, D. Chen, J. Li, J. Xu, J. Lv, H. Liu and Y. Li, *Org. Lett.*, 2007, **9**, 3929-3932.
7. B. Baytekin, S. S. Zhu, B. Brusilowskij, J. Illigen, J. Ranta, J. Huuskonen, L. Russo, K. Rissanen, L. Kaufmann and C. A. Schalley, *Chem. Eur. J.*, 2008, **14**, 10012-10028.
8. K. Hirose, *J. Inclusion Phenom. Macrocyclic Chem.*, 2001, **39**, 193-209.
9. K. Hirose, in *Analytical Methods in Supramolecular Chemistry*, Wiley-VCH Verlag GmbH & Co. KGaA, 2012, DOI: 10.1002/9783527644131.ch2, pp. 27-66.
10. S. Richter, J. Poppenberg, C. H. H. Traulsen, E. Darlatt, A. Sokolowski, D. Sattler, W. E. S. Unger and C. A. Schalley, *J. Am. Chem. Soc.*, 2012, **134**, 16289-16297.
11. J. Poppenberg, S. Richter, C. H. H. Traulsen, E. Darlatt, B. Baytekin, T. Heinrich, P. M. Deutinger, K. Huth, W. E. S. Unger and C. A. Schalley, *Chem. Sci.*, 2013, **4**, 3131-3139.
12. S. Richter, C. H. H. Traulsen, T. Heinrich, J. Poppenberg, C. Leppich, M. Holzweber, W. E. S. Unger and C. A. Schalley, *J. Phys. Chem. C*, 2013, **117**, 18980-18985.

13. C. H. H. Traulsen, V. Kunz, T. Heinrich, S. Richter, M. Holzweber, A. Schulz, L. K. S. von Krbek, U. T. J. Scheuschner, J. Poppenberg, W. E. S. Unger and C. A. Schalley, *Langmuir*, 2013, DOI: 10.1021/la403222x.
14. T. Heinrich, C. H. H. Traulsen, E. Darlatt, S. Richter, J. Poppenberg, N. L. Traulsen, I. Linder, A. Lippitz, P. M. Dietrich, B. Dib, W. E. S. Unger and C. A. Schalley, *RSC Adv.*, 2014, **4**, 17694-17702.
15. T. Heinrich, C. H. H. Traulsen, M. Holzweber, S. Richter, V. Kunz, S. K. Kastner, S. O. Krabbenborg, J. Huskens, W. E. S. Unger and C. A. Schalley, *J. Am. Chem. Soc.*, 2015, **137**, 4382-4390.
16. G. T. Carroll, G. b. London, T. F. n. Landaluce, P. Rudolf and B. L. Feringa, *ACS Nano*, 2011, **5**, 622-630.